Responses to the Anonymous Referee-1 comments

Referee #1 Evaluations:

The comments on "Characterization of organic aerosols from a Chinese Mega-City during winter: predominance of fossil fuel combustion" submitted by Haque et al. In this study, PM2.5 samples were collected from an urban site in Nanjing, a big city in East China. A comprehensive laboratory analysis was conducted for various organic compounds. Based on the characteristics of different organic compounds, and also the PMF receptor model, the sources of organic aerosols were identified. General speaking, this work has value for the mitigation of the serious air pollution in China. However, this paper suffers some major problems, regarding the writing and organization.

Response: We thank the reviewer for the nice summary of our paper and the positive assessment of this work. We have carefully revised the manuscript following the reviewer's comments and suggestions. Our responses to all comments made by the reviewer are given below. Please refer to the revised MS, in which changes are highlighted in yellow.

Specific comments:

1. Line 55-60, I do agree that organic aerosols are important in the climate system, as CCN. However, I can not understand why the authors use another whole paragraph (Line 78-95) to describe this issue repeatedly and in such detailed way. Actually, for the urban sites, the aerosol is more closely related to the pollution (environmental) issue, rather than climate issue. Obviously, the role of organic aerosols in the climate is not the focus of this study.

Response: Considering the reviewer's comment, we removed the paragraph and revised this section. Please see lines 55-57 and 70-72 in the revised MS.

2. Line 100-101, the references cited here seem too old. In the recent years, many research was conducted in terms of inorganic aerosols like sulfate and nitrate from anthropogenic emissions, rather than desert dust.

Response: Following the reviewer's suggestions, we have cited recently published papers. Please see lines 91-94 in the revised MS.

3. Line 105-108, what is the current status of air quality in Nanjing? What is the concentration level of PM2.5 during the sampling time? Updated information and reference should be presented here. Also, the China national standard of air quality or WHO standard should be used here.

Response: The average concentrations of $PM_{2.5}$ were 66±33 μg m^{-3} in Nanjing aerosols during sampling period, whereas the Chinese Ambient Air Quality and WHO standard levels are 35 μg m^{-3} and 25 μg m^{-3}, respectively (Liu et al., 2016; Shen et al., 2014), indicating that Nanjing air quality is still worse compared to China national and WHO standard levels. Please see lines 100-104 in the revised MS.

4. Line 111, Why winter season was selected for the sampling? What is the special characteristics of winter compared to other seasons?

Response: The highest $PM_{2.5}$ concentrations were observed during winter in China due to the enhancement of anthropogenic emissions from fossil fuel combustion and biomass burning and unfavorable meteorological conditions, i.e., frequent development of inversion layers

(Zhang et al., 2015). Ma et al. (2016) also reported PM$_{2.5}$ concentrations from 2004-2013 in China while winter was the most polluted season. Please see lines 105-109 in the revised MS.

5. In the Experimental section, major ions should be included. Because ions data were used in this study, especially in the PMF analysis, soil dust (indicated by Ca2+) was identified as the Factor 2.
Response: Following the reviewer's recommendations, we included the analysis of major ions in the experimental section. Please see lines 197-209 in the revised MS.

6. Line 245, it was written as "The OC/EC ratio in this study was on average 2.40, suggesting the significant contribution of SOA in Nanjing aerosols". Actually, there are other possible causes. First, as the OC/EC ratio of coal combustion is 2.7, which was proposed by Watson 2001(Line 236), so only coal combustion rather than secondary formation could produce the ratio of 2.4 here. I do not think the ratio is high. Maybe sometime the ratio for vehicular emission is low, but when it was mixed by biomass-burning emission (as discussed latter), the ratio also could increase somewhat.
Response: We agree with reviewer's opinion. Based on the OC/EC ratio, we made conclusion that fossil fuel combustion is the major source of carbonaceous aerosols in Nanjing (please see lines 254-255 in the revised MS). However, SOA may also be important in Nanjing aerosols, which was discussed based on the air mass trajectories, WSOC/OC ratio and source contribution. Please see lines 256-268 in the revised MS.

7. Line 277-278, some sentence seem missing here. What is the situation found in this study?
Response: We have removed these lines because we have used CPI values for the source indicator either it is fossil fuels or biogenic. Please see lines 292-302 in the revised MS.

8. Line 346-350. The amount of galactosan was found to be 0.65-7.47 ng m-3 (ave. 2.26 ng m-3) during daytime and 0.48–7.75 ng m-3 (3.13 ng m-3) during nighttime, whereas those of mannosan were 0.36-4.30 ng m-3 (1.62 -349 Ăang m-3) in daytime and 0.27-5.73 ng m-3 (2.06 ng m-3) in nighttime. Galactosan and mannosan were also detected in the aerosol samples. Please check the logic among these sentences.
Response: We have restructured these lines. Please see lines 359-363 in the revised MS.

9. Line 422, why the coal combustion should be higher in nighttime? Any references or supporting information?
Response: Households coal combustion has a significant contribution to ambient air quality in China during winter (Kerimray et al., 2017). Temperature falls down during nighttime resulting in the uses of a large amount of coal for house heating in a rural area due to the cold weather. Based on the reviewer's comments, we have included these points in the revised MS. Please see lines 432-435 in the revised MS.

10. Line 428-430, I suggest to delete these sentence here. Because the sources of PAHs were discussed more detailed in the below (Line 442-453) using the PAHs ratios.
Response: Deleted.

11. Does the dataset (data amount) meet the requirement of PMF?
Response: Yes, the dataset meets the requirement of PMF. There is no specific number of samples for PMF analysis (Hopke et al., 2010). However, a large number of samples can give less uncertainty and stable PMF results. PMF source apportionment relies on source specific

species to explore ambient pollution sources. In this study, we observed distinguishably different source profiles using PMF analyses.

12. Sometime, the authors attribute the source of pollutants to long-range transport (e.g. Line 650). Actually, most of emission information provided in the text is the local emission pattern, like local truck.

Response: We found higher concentrations of secondary oxidation products in nighttime rather than daytime when photochemical oxidation was absent. We have proposed two explanations for the higher concentrations of SOA products during nighttime. First, SOA products might be formed during long-range atmospheric transport that is consistent with aged PAHs and high OC/EC and WSOC/OC ratios in the Nanjing aerosols (please see lines 256-268, 442-452 in the revised MS). The back trajectories also indicate long-range transport while some air masses come from the polluted regions over North China (please see below figure). Second, NOx can play an important role to form SOA products in nighttime when NOx concentration is high. Please see lines 561-573, 598-601, and 660-662 in the revised MS.
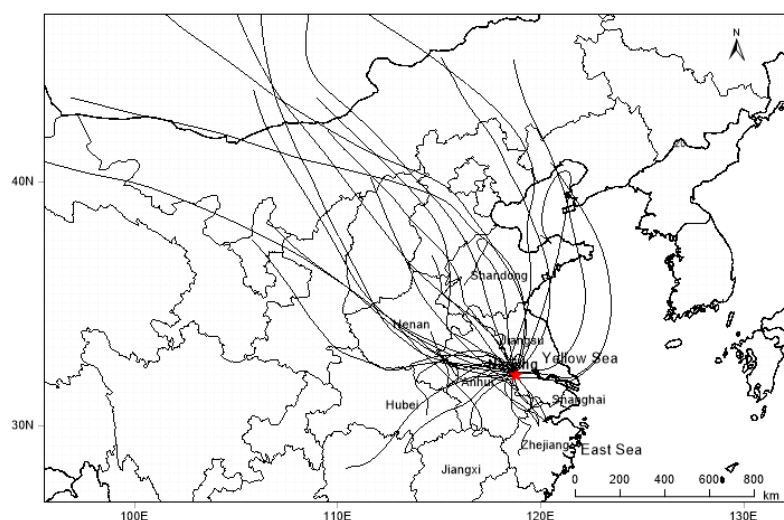
Figure: 48 hrs backward air mass trajectories arriving at 500 m above the ground level to Nanjing, China during 11 Dec 2014–11 Jan 2015.

References

Chang, Y., Zhang, Y., Tian, C., Zhang, S., Ma, X., Cao, F., Liu, X., Zhang, W., Kuhn, T., and Lehmann, M. F.: Nitrogen isotope fractionation during gas-particle conversion of NOx to NO_3^- in the atmosphere – implications for isotope-based NOx source apportionment, Atmos. Chem. Phys., 18, 11647-11661, https:// doi.org/ 10.5194/acp-18-11647-2018, 2018.

Fu, P. Q., Kawamura, K., Pavuluri, C. M., Swaminathan, T., and Chen, J.: Molecular characterization of urban organic aerosol in tropical India: contributions of primary emissions and secondary photooxidation, Atmos. Chem. Phys., 10(6), 2663–2689, 2010.

Hopke, P. K.: Discussion of "Sensitivity of a molecular marker based positive matrix factorization model to the number of receptor observations" by Yuan Xun Zhang, Rebecca J. Sheesley, Min-Suk Bae and James J. Schauer., Atmos. Environ. 44 (8), 1138, 2010.

Kawamura, K., Ishimura, Y., and Yamazaki, K.: Four years' observations of terrestrial lipid class compounds in marine aerosols from the western North Pacific, Glob. Biogeochem. Cycles,. 17, 1003(1), doi:10.1029/2001GB001810, 2003.

Kerimray, A., Luis, R.-S., Torkmahalleh, M. A., Hopke, P. K., Gallachóir, B. P. Ó.: Coal use for residential heating: Patterns, health implications and lessons learned, Ener. Sus. Devlop., 40, 19–30, 2017.

Liu, J., Han, Y., Tang, X., Zhu, J., and Zhu, T: Estimating adult mortality attributable to $PM_{2.5}$ exposure in China with assimilated $PM_{2.5}$ concentrations based on a ground monitoring network. Sci. Total Environ., 568, 1253–1262. doi:10.1016/j.scitotenv. 2016.05.165, 2016.

Ma, Z., Hu, X., Sayer, A. M., Levy, R., Zhang, Q., Xue, Y., Tong, S., Bi, J., Huang, L., Liu, Y.: Satellite-based spatiotemporal trends in $PM_{2.5}$ concentrations: China, 2004–2013, Environ. Health Perspect., 124, 184–192, http://dx.doi.org/10.1289/ehp.1409481, 2016.

Shen, G. F., Yuan, S. Y., Xie, Y., Xia, S. J., Li L., Yao, Y. K., Qiao, Y. Z., Zhang, J., Zhao, Q. Y., Ding, A. J., Li, B., and Wu, H. S: Ambient levels and temporal variations of $PM_{2.5}$ and PM_{10} at a residential site in the mega-city, Nanjing, in the western Yangtze River Delta, China, J. Environ. Sci. Health, Part A 49, 171–178, 2014.

Simoneit, B. R. T., Cardoso, J. N., and Robinson, N.: An assessment of terrestrial higher molecular weight lipid compounds in aerosol particulate matter over the south Atlantic from about 30-70º S, Chemosphere, 23(4), 447–465, 1991.

Wang, G., and Kawamura, K.: Molecular characteristics of urban organic aerosols from Nanjing: A case study of a mega-city in China, Environ. Sci. Technol., 39(19), 7430–7438, 2005.

Zhang, Y., and Cao, F.: Fine particulate matter ($PM_{2.5}$) in China at a city level, Scientific Reports, 2015 DOI: 10.1038/srep14884

1 **Characterization of organic aerosols from a Chinese Mega-City during winter: predominance of fossil fuel combustion**

4 **Md. Mozammel Haque[1,2,3], Kimitaka Kawamura[2], Dhananjay K. Deshmukh[2], Cao**

5 **Fang[1, 3], Wenhuai Song[1,3], Bao Mengying[1,3] and Yan-Lin Zhang[1,3*]**

7 *[1] Yale-NUIST Center on Atmospheric Environment, Department of Applied*

8 *Meteorology, Nanjing University of Information Science and Technology, Nanjing*

9 *210044, China*

10 *[2] Chubu Institute for Advanced Studies, Chubu University, Kasugai 487-8501, Japan*

11 *[3]Key Laboratory of Meteorological Disaster, Ministry of Education & Collaborative*

12 *Innovation Center on Forecast and Evaluation of Meteorological Disasters, Nanjing*

13 *University of Information Science and Technology, Nanjing 210044, China*

16 *Corresponding author*

17 Yan-Lin Zhang

18 E-mail: dryanlinzhang@outlook.com

20 2 March, 2019

Abstract

PM$_{2.5}$ aerosol samples were collected from a Chinese mega-city in Nanjing (32.21°N and 118.73°E) during winter and analyzed for more than 100 compounds of twelve organic compound classes. The most abundant classes of compounds are *n*-alkanes (average, 205 ng m^{-3}), followed by fatty acids (76.3 ng m^{-3}), polycyclic aromatic hydrocarbons (PAHs) (64.3 ng m^{-3}), anhydro-sugars (56.3 ng m^{-3}), fatty alcohols (40.5 ng m^{-3}), and phthalate esters (15.2 ng m^{-3}), whereas hydroxy-/polyacids (8.33 ng m^{-3}), aromatic acids (7.35 ng m^{-3}), hopanes (4.19 ng m^{-3}), primary sugars and sugar alcohols (4.15 ng m^{-3}), lignin and resin products (2.94 ng m^{-3}), and steranes (2.46 ng m^{-3}) are less abundant. The carbon preference index of *n*-alkanes (0.83-1.38) indicated that they were significantly originated from the fossil fuels combustion. Diagnostic concentration ratios of organic tracers suggested that PAHs and hopanes are mostly originated from coal burning and traffic emissions, respectively in Nanjing urban area. Positive matrix factorization analysis demonstrated that fossil fuel combustion is the major source (28.7%) in Nanjing winter aerosols. Most of the compounds generally showed higher concentrations in nighttime compared to daytime, due to the accumulation process associated with the inversion layers and enhancement of emissions from heavy trucks at night. We conclude that fossil fuel combustion largely influences the winter organic aerosols in urban Nanjing area. Based on the comparison of present results with previous studies, we found that pollution levels on organic aerosols have been decreased in the urban Nanjing atmosphere for the last decade.

Keywords: PM$_{2.5}$, organic compounds, fossil fuel combustion, positive matrix factorization, Chinese urban aerosols.

1 Introduction

Particulate matter (PM) comprised a wide variety of chemical components, which are derived from a broad range of sources and processes in the atmosphere (Seinfeld and Pandis, 2006). Organic aerosol (OA) is one of the major constituents of airborne particulates, accounting for up to 70% of the fine aerosol mass. They can play a crucial role in the radiative forcing of the Earth and more generally to the environment (Kanakidou et al., 2005). In the last two decades, more attention has been paid to identify organic aerosol optical and cloud formation properties that link OA directly to hydrological cycle and thereby sustainability issues (Dusek et al., 2006; Riipinen et al., 2012). They can affect the climate, air quality, human health, visibility, and ecosystems on the local, regional and global scale (Salma et al., 2017). Several studies have reported that OA plays an important role in both the direct and indirect aerosol forcing, affecting the earth's radiation balance and global air quality (Cooke et al., 1999; Lohmann et al., 2000; Jacobson, 2001; Chung and Seinfeld, 2002). Aerosol particles improved with OM can make the aerosol surfaces more hydrophilic or hydrophobic based on the mixing state and aerosol composition, which further modify the CCN activities of particles. Furthermore, aerosols also influence air quality in addition to human health and climate, particularly in urban areas due to extensive anthropogenic emissions and favorable meteorological conditions (Watson, 2002).

There are two major sources of atmospheric aerosols that include both primary emissions and secondary aerosol formation. Primary organic aerosols (POA) are directly derived from various sources such as biomass burning, fossil fuels combustion, dust particles, microbial activities, and plant materials, etc., whereas secondary organic aerosols (SOA) are formed by the oxidation process of organic species in the atmosphere. Various types of volatile organic compounds (VOCs) are emitted from

natural and anthropogenic sources into the atmosphere. VOCs can be further photo-oxidized by OH, NO_x, O_3 to form SOA in the atmosphere (Haque et al., 2016). Both POA and SOA can contribute to the organic particulate matter (PM) formation in the atmosphere, which can significantly control the physicochemical properties of aerosol particles (Kanakidou et al., 2005). The chemical characterization and the contributions of various sources of aerosol particles are essential to figure out the role and potential impacts of OA in the atmosphere. Moreover, OA poses adverse physiological effects on human health causing asthma, bronchitis, cancer, and heart disease, etc. (Pope et al., 2009; Ramírez et al., 2011).

The large emissions of atmospheric particles from China have a major effect on regional and global climate changes (Huebert et al., 2003). Atmospheric pollution in China is a serious problem due to its rapid industrialization and urbanization. Globally, one-fourth of anthropogenic POA are originated in China (Cooke et al., 1999). Many studies have been performed to characterize inorganic aerosols from China due to the significant anthropogenic emissions. (Wang et al., 2011; He et al., 2012; Zheng et al., 2015; Li et al., 2017). However, studies on OAs of Chinese mega-cities are still poorly understood (Guo et al., 2003; Bi et al., 2003; Yao et al., 2003). Nanjing is a highly industrialized mega-city located in east China with a population of over 8 million where air pollution is a critical problem. Previous studies of Wang et al. (2002a; 2002b) reported that the aerosol mass of fine particles (< 2.5 µm) in Nanjing atmosphere was about 2-4 times higher than the United States Environmental Protection Agency (USEPA) regulations. The average concentrations of $PM_{2.5}$ were 66±33 µg m^{-3} in Nanjing aerosols during sampling period, whereas the Chinese Ambient Air Quality and WHO standard levels are 35 µg m^{-3} and 25 µg m^{-3}, respectively (Liu et al., 2016; Shen

et al., 2014), indicating that Nanjing air quality is still worse compared to China national and WHO standard levels.

The highest $PM_{2.5}$ concentrations were observed during winter in China due to the enhancement of anthropogenic emissions from fossil fuel combustion and biomass burning and unfavorable meteorological conditions, i.e., frequent development of inversion layers (Zhang et al., 2015). Ma et al. (2016) also reported $PM_{2.5}$ concentrations from 2004-2013 in China while winter was the most polluted season. To better understand the molecular composition and sources of OAs in Chinese urban area during winter, aerosol sampling campaign was carried on a day and night basis in the mega-city of Nanjing during winter period from 11 December 2014 to 11 January 2015. The objective of this study is to determine more than 100 organic compounds including aliphatic lipids, sugar compounds, polycyclic aromatic hydrocarbons (PAHs), hopanes, lignin and resin products, aromatic acids, polyacids, and steranes in the aerosol particles from Nanjing. Their chemical characteristics, diurnal patterns, and potential sources are discussed in comparison with previous studies conducted a decade ago.

2 Experimental

2.1 Sample collection

$PM_{2.5}$ sampling was performed from the rooftop of a six-story building at Nanjing University of Information Science and Technology, Nanjing, China using medium volume sampler (Laoshan, Quingdao, China) from 11 December 2014 to 11 January 2015 (Figure 1). Daytime and nighttime sampling was conducted from 9:30 to 21:00 and 21:30 to 9:00, respectively. Total of 62 samples was collected on prebaked (450°C for 6 h) quartz fiber filters (80 mm) with an air flow rate of 100 L min^{-1}. After sampling, the filter samples were wrapped with aluminum foil, transported to the laboratory and stored at -20°C until the analysis.

2.2 Analysis of polar organics

Several polar organic compounds containing COOH and OH groups were analyzed by gas chromatography-mass spectrometry (GC-MS) using solvent extraction followed by TMS-derivatization technique (Table S1). Filter aliquots (6.28 cm^2) were extracted three times with 5 mL of dichloromethane/methanol mixture (2:1) under ultra-sonication for 10 min. The solvent extracts were filtered through quartz wool packed in a Pasteur pipette to remove all insoluble matrixes, concentrated using a rotary evaporator under vacuum and then totally dried under a gentle nitrogen stream. The dried extracts were derivatized with 50 µL of N,O-bis-(trimethylsilyl)trifluoroacetamide (BSTFA) plus 1% trimethylsilyl chloride and 10 µL of pyridine in a glass vial (1.5 mL) with a Teflon-lined screw cap at 70°C for 3h. The C$_{13}$ n-alkane (diluted in n-hexane) was used as an internal standard (1.43 ng µL^{-1}) prior to injection into a GC-MS for identification. Detailed information on the chemical analysis is interpreted elsewhere (Wang and Kawamura, 2005).

The derivatives were analyzed using Hewlett-Packard (HP) model 6890 GC coupled to an HP model 5973 mass-selective detector (MSD). The sample was injected into a splitless mode with the injector temperature at 280°C. The GC oven temperature was set at 50°C for 2 min and then increased from 50 to 120°C at 30°C min^{-1}, and then to 300°C at 6°C min^{-1} with a final isothermal hold at 300°C for 16 min. The GC separation was performed on a DB-5MS fused silica capillary column (30 m long × 0.25 mm inner diameter × 0.5 µm film thickness) with a carrier gas of helium (rate 1.0 mL min^{-1}). The mass spectrometer was conducted at 70 eV on an electron impact (EI) mode with a scan range from 50 to 650 Daltons (Da).

The organic components were determined by comparison with the retention times and mass spectra of authentic standards as well as literature and National Institute

153 of Standards and Technology (NIST) library data of mass fragmentation patterns

154 (Medeiros and Simoneit, 2007). GC-MS relative response factor (RRF) of each

155 compound was calculated using authentic standards and surrogate compounds. We

156 performed a recovery experiment three times and acquired the average value of more

157 than 80% for target compounds. The field blank filters (n = 5) were analyzed by the

158 procedures as described above. The target species were not noticed in the blank filters.

159 The analytical errors based on replicate analyses (n = 5) were <10%.

160 **2.3 Analysis of nonpolar organics**

161 Non-polar organics, including n-alkanes, PAHs, hopanes, and steranes were

162 analyzed using thermal desorption gas chromatography-mass spectrometry (TD-GC-

163 MS) technique. It should be noted that higher recoveries (>90%) were obtained for

164 nonpolar organics using TD-GC-MS compared to TMS-derivatization/GC-MS (<70%)

165 technique. The filter aliquots (3 mm diameter) were cut into two pieces and then placed

166 into a TD quartz tube (78 mm long × 4 mm inner diameter) and spiked with internal

167 standard mixture (isotope-labeled reference compounds) for quantification. The internal

168 standards consisted of 3 deuterated PAHs, e.g., Nap-d_8, Ace-d_{10}, and Phe-d_{10}.

169 Thermal desorption was performed on an Agilent GC-MS system model

170 7890B/5977A. A capillary column (HP-5MS UI, 5% biphenyl/95% dimethylsiloxane,

171 30 m long × 0.25 mm inner diameter × 0.25 µm film thickness) was used to separate the

172 target compounds. The GC oven temperature programmed from 35°C (3 min) to 120°C

173 at 10°C min^{-1}, ramped from 120°C to 146°C at 4°C min^{-1} and continued to 310°C at

174 8°C min^{-1}, then held at 310°C for 16 min. The sample on the filter punch was inserted

175 into the TD tube with the initial temperature at 35°C before running and increased up to

176 300°C manually at 12°C sec^{-1} after starting the analysis. Column flow rate was 2 mL

177 min^{-1} and split flow was 10 mL min^{-1} for the first 3 mins, then column and split flow

178 rate changed to 1 mL min^{-1} and 25 mL min^{-1}, respectively. The electron ionization mass

179 spectra (70 eV) were conducted on a scan mode range from 50 to 650 Da. The

180 temperatures of the ion source, quadruples and transfer line were set at 310, 150 and

181 310°C, respectively.

2.4 Carbonaceous components analysis

183 Organic carbon (OC) and elemental carbon (EC) were measured using a Sunset

184 Laboratory carbon analyzer following the IMPROVE (Interagency Monitoring of

185 Protected Visual Environments) thermal-optical evolution protocol and assuming

186 carbonate carbon to be insignificant in the sample (Boreddy et al., 2018). An area of

187 1.54 cm^2 of each quartz filter sample was insert in a quartz boat inside the thermal

188 desorption chamber of the analyzer, and then stepwise heating was performed.

189 A filter cut of 3.14 cm^{2}of each sample was extracted with 20 mL organic-free

190 ultrapure water (resistivity >18.2 MΩ cm, Sartorius arium 611 UV) under

191 ultrasonication for 30 min. The water extracts were then passed through a membrane

192 disc filter to throw away the insoluble filter matrixes and analyzed for water-soluble

193 organic carbon (WSOC) using a total organic carbon (TOC) analyzer (Shimadzu, TOC-

194 Vcsh) (Boreddy et al., 2018). The analytical errors in the triplicate analyses were within

195 5% for all carbonaceous components and the concentrations reported here were

196 corrected for the field blanks.

2.5 Major inorganic ion analysis

198 An area of 5.07 cm^2 of each quartz filter sample was extracted with 10.0 mL

199 ultrapure water (> 18.2 Ω) under ultrasonication (30 min). The extract solution was

200 filtered through a membrane disc filter (Millex-GV, Millipore) of pore size 0.22 μm to

201 remove insoluble materials, then analyzed for inorganic ions using ion chromatography

202 on a Thermo Fisher Scientific ICS-5000 (America) equipped with a gradient pump

3 Results and Discussion

3.1 Diurnal variations and meteorological conditions

No significant difference was observed between day- and night-time for organic compounds in winter aerosols from Nanjing urban area (Figure 2, Tables 1 and S1). Nevertheless, concentrations of organic compounds in nighttime were slightly higher than daytime in most of the cases. It is notable that the planetary boundary layer height (PBLH) is generally lower in nighttime than daytime causing higher concentrations of aerosol particles at night. Interestingly, we found high loadings of organics in daytime sample collected on 15 December when PBLH was high (632 m), whereas lower levels of organics were observed in nighttime of 14 December (PBLH = 82.2 m) (Figures 3 and S1b).

We observed one episode (E1) during 2 - 5 January while PM$_{2.5}$ and all organic compounds showed similar temporal variations with high loadings (Figure 3). Fascinatingly, NO$_2$ showed high concentration during E1, whereas relative humidity (RH) and ozone (O$_3$) levels were not high (Figure S1). Our results suggest that NO$_2$ influences the organic molecular compositions in urban aerosols. It is noteworthy that the major source of NO$_2$ is of vehicular exhaust origin (Kendrick et al., 2015). However, coal combustion can also emit NOx into the atmosphere (Chang et al., 2018).

228 Previous studies also reported that NO_x could affect SOA formation (Kanakidou et al.,

229 2005; Zhang et al., 2015; Mochizuki et al., 2015). Moreover, PAHs, hopanes, and

230 steranes showed another episode on 23 and 24 December 2014 probably due to the coal

231 combustion event. It should be noted that higher RH (81-88%) and $PM_{2.5}$ levels (152-

232 226 µg m^{-3}) cause less visibility on 29 December (1.7 km), 10 January (1.8 km), and 11

233 January (1.6 km), which might be due to the haze formation. It is remarkable that the

234 levels of organics were not high during these periods (Figures 3 and S1). These results

235 imply that NO_2 derived from fossil fuel combustion plays an important role in the

236 formation of OAs in the Nanjing atmosphere.

237 **3.2 Carbonaceous components**

238   The results of OC, EC, and WSOC are mentioned in Table 1. The values of OC

239 and EC were found to be 8.76-40.0 µg m^{-3} (ave. 18.6 µg m^{-3}) and 2.41-30.3 µg m^{-3} (8.25

240 µg m^{-3}) in daytime, and 2.98-40.1 µg m^{-3} (19.1 µg m^{-3}) and 0.87-22.9 µg m^{-3} (8.86 µg

241 m^{-3}) in nighttime, respectively. We found that the day and night variations of OC and

242 EC values are also not significant. The mass ratio of OC to EC (OC/EC) is often used to

243 characterize fossil fuels and biomass burning emissions. Several investigators have used

244 OC/EC ratios to classify the sources of carbonaceous aerosols (Ram et al., 2008;

245 Sandradewi et al., 2008; Saarikoski et al., 2008). The higher OC/EC ratios imply that

246 major source of carbonaceous species is from biomass burning, whereas lower ratios are

247 characteristics of emissions from fossil fuels combustion. Sandradewi et al. (2008) have

248 documented an average OC/EC ratio of 1.1 for vehicular emission and 7.3 for wood

249 burning emission. Saarikoski et al. (2008) pointed out OC/EC ratios of 0.71 for

250 vehicular emission and 6.6 for biomass burning. Watson et al. (2001) proposed the

251 OC/EC ratios of 1.1 for vehicular emission, 2.7 for coal combustion and 9.0 for biomass

252 burning emission. The OC/EC ratios ranged from 1.30 to 3.80 with a mean value of

253 2.40 in this study, which is comparable to the values reported for coal combustion and

254 vehicular emission. These results suggest that fossil fuel combustion is the major source

255 of carbonaceous aerosols in urban Nanjing.

256 The ratios of OC to EC are also used to differentiate the relative contribution of

257 primary vs. secondary sources; high OC/EC ratios (>2.0) were reported for the aerosols

258 with significant contributions of SOA (Kunwar and Kawamura, 2014; Pani et al., 2017).

259 The OC/EC ratio in this study was on average 2.40, suggesting the significant

260 contribution of SOA in Nanjing aerosols that is consistent with PMF results (see section

261 3.4). The concentration range of WSOC was 5.52-26.6 $\mu g\ m^{-3}$ (11.7 $\mu g\ m^{-3}$) in daytime

262 and 2.51-20.2 $\mu g\ m^{-3}$ (11.8 $\mu g\ m^{-3}$) in nighttime. The WSOC/OC ratios often used to

263 discuss the SOA formation via photochemical aging of atmospheric aerosol particles.

264 The WSOC/OC ratios exceeding 0.4 indicate the aged aerosols with the significant

265 contribution of SOA (Boreddy et al., 2018). The average WSOC/OC ratio of 0.64 in the

266 present study indicates that OAs in Nanjing were relatively aged**.** Moreover, air mass

267 back trajectories also indicate that some air masses come from the polluted regions over

268 North China, suggesting a SOA formation during long-range transport (Figure S5).

269 **3.3 Organic molecular compositions**

270 We detected twelve organic compound classes, including sugars, lignin and

271 resin acids, fatty acids, fatty alcohols, *n*-alkanes, PAHs, hopanes, steranes, glycerol and

272 polyacids, phthalate esters, and aromatic acids in the aerosol samples from Nanjing. The

273 total concentrations of organics were on average 424 ng m^{-3} in daytime and 555 ng m^{-3}

274 in nighttime with the predominance of *n*-alkanes followed by fatty acids, PAHs,

275 anhydro-sugars, fatty alcohols, phthalate esters, glycerol and polyacids, aromatic acids,

276 sugars, hopanes, lignin and resin acids, and steranes (Figure 2). Table S1 shows the

277   values of identified organic compounds. Levoglucosan was the single dominant species

278   followed by C_{16} and C_{24} fatty acids, and C_{29} *n*-alkane (Table S1).

279   **3.3.1 Aliphatic lipid components**

280   The lipid compounds, e.g., fatty acids, fatty alcohols, and *n*-alkanes are mainly

281   originated from marine or microbial detritus, terrestrial higher plant waxes, and fossil

282   fuels combustion. Homologues of *n*-alkanes (C_{13}-C_{39}) were detected with higher

283   concentrations in nighttime (74.8-535 ng m^{-3}, ave. 228 ng m^{-3}) than daytime (97.6-497

284   ng m^{-3}, 184 ng m^{-3}) with a maximum at C_{29} (14.0 ng m^{-3} during daytime and 17.9 ng m^{-3}

285   during nighttime) in Nanjing aerosols (Tables 1 and S1, Figure 4a). These

286   concentrations are comparable to those reported from urban cities in Hong Kong (195

287   ng m^{-3}) and Shanghai (259 ng m^{-3}) (Wang et al., 2006), but much higher than the

288   western North Pacific region (0.11-14.1 ng m^{-3}) (Kawamura et al., 2003). Concentration

289   levels of *n*-alkanes in this study are not significantly different from previous studies in

290   Nanjing (112-265 ng m^{-3}, 172 ng m^{-3} during daytime; 61.0-503 ng m^{-3}, 278 ng m^{-3}

291   during nighttime) (Table 2) (Wang and Kawamura, 2005).

292   Biogenic *n*-alkanes showed stronger odd/even carbon number predominance

293   with a carbon preference index (CPI) of >5, whereas anthropogenic *n*-alkanes CPI value

294   is usually close to unity (Simoneit et al., 1991a, 2004c). CPI values obtained in this

295   study ranged from 1.18-1.32 (ave. 1.28) in daytime and 1.10-1.37 (1.24) in nighttime,

296   which is close to unity. This result suggests that the major contributor of *n*-alkanes is

297   the anthropogenic activity such as fossil fuels combustion with less contribution from

298   higher plants in Nanjing aerosols. The present CPI values are similar with those from

299   other Chinese urban areas (ave. 1.16) (Wang et al., 2006) and Tokyo (1.10-2.80, ave.

300   1.50) (Kawamura et al., 1995). On the contrary, higher CPI values were reported for

301   Mt. Tai (4.60) (Fu et al., 2008) and Chichi-jima aerosols (4.50) (Kawamura et al.,

2003), where *n*-alkanes were mainly originated from terrestrial higher plant waxes. Plant wax derived *n*-alkanes are estimated as the excess of odd homologues minus adjacent even homologues (Simoneit et al., 1991b, 2004c), which is attributable to vascular plant waxes (Tables 1 and S1). Concentrations ranges of higher plant wax derived *n*-alkanes were 2.12-48.1 ng m^{-3} (ave. 15.5 ng m^{-3}) in daytime and 0.86-58.9 ng m^{-3} (17.6 ng m^{-3}) in nighttime, both of which are much lower than total *n*-alkanes, indicating that *n*-alkanes in Nanjing urban area are derived mainly from fossil fuel combustion.

A homologous series of $C_{12:0}$-$C_{32:0}$ saturated fatty acids, including two unsaturated fatty acids ($C_{18:1}$ and $C_{18:2}$), were identified in Nanjing samples. The values of total fatty acids ranged from 14.3 to 254 ng m^{-3} (ave. 66.8 ng m^{-3}) during daytime, whereas they ranged from 8.59 to 252 ng m^{-3} (91.3 ng m^{-3}) during nighttime. It is notable that fatty acids are less abundant compared to *n*-alkanes in Nanjing samples (Figure 2). The molecular distributions of fatty acids are observed by a strong even carbon number predominance with C_{max} at $C_{16:0}$ and $C_{24:0}$ (Table S1 and Figure 4b). CPI values of fatty acids are found to be 5.41 in daytime and 5.52 in nighttime samples. A similar distribution pattern has been proposed in marine and continental aerosols (Mochida et al., 2002; Kawamura et al., 2003; Fu et al., 2008). LMW fatty acids ($<C_{20:0}$) are originated from various sources, e.g., vascular plants, microbial sources, and marine phytoplankton, while HMW fatty acids ($>C_{20:0}$) are derived from terrestrial higher plant waxes (Kawamura et al., 2003; Kolattukudy, 1976; Simoneit, 1978). Biomass burning, motor vehicles, and cooking can also be the important sources of fatty acids in urban areas (Fu et al., 2010). The values of $C_{18:1}$ was observed lower in daytime than nighttime, suggesting an enhanced emission to the atmosphere and oxidation with a higher rate in daytime (Kawamura and Gagosian, 1987).

327   Concentration ranges of C_{12}-C_{34} fatty alcohols were 7.30-165 ng m^{-3} (ave. 36.9

328   ng m^{-3}) during daytime and 4.61-129 ng m^{-3} (43.8 ng m^{-3}) during nighttime (Table S1

329   and Figure 2). Their molecular distributions are characterized by a strong even-to-odd

330   carbon number predominance with C_{max} at C_{28} or C_{30} (Figure 4c). We found that the

331   CPI values of fatty alcohols in Nanjing aerosols (2.56-10.3, ave. 5.22 in daytime and

332   3.06-15.5, 6.32 in nighttime) are lower than those of aerosols from Chennai, India

333   (9.75±2.94) (Fu et al., 2010) and Mt. Tai, China (CPIs 7.95-66.5, ave. 25.6 in daytime

334   and 12.2-53.4, 22.8 in nighttime) (Fu et al., 2008). HMW fatty alcohols ($>C_{20}$) are

335   dominant in the terrestrial higher plant, soils, and loess deposits, whereas LMW fatty

336   alcohols ($<C_{20}$) are dominant in marine biota and soil microbes (Simoneit et al., 1991b).

337   Moreover, a large amount of fatty alcohols together with fatty acids and n-alkanes can

338   also be derived from biomass burning (Simoneit, 2002). A positive correlation was

339   observed between fatty alcohols and levoglucosan (r = 0.60, p<0.001), indicating that

340   fatty alcohols are partly originated from biomass burning in Nanjing winter aerosols

341   (Figure S2c). This conclusion is further supported by the factors resolved by PMF

342   analysis, where high loading of fatty alcohols was found with a biomass burning tracer

343   levoglucosan.

344   **3.3.2 Biomass burning tracers**

345   Levoglucosan, galactosan, and mannosan are class of anhydro-sugars, which are

346   produced by the pyrolysis of cellulose and hemi-cellulose (Simoneit, 2002).

347   Levoglucosan is a unique tracer of biomass burning, and has been reported in urban

348   (Wang et al., 2006; Fu et al., 2010; Yttri et al., 2007), marine (Simoneit et al., 2004b;

349   Ding et al., 2013), and polar regions (Stohl et al., 2007; Fu et al., 2009). Levoglucosan

350   is a relatively stable species in the atmospheric aerosol and could be transported long

351   distances (Mochida et al., 2010). We found that levoglucosan is one of the most

abundant single tracer among all the identified compounds in the presents study, with a

concentration range of 4.79-179 ng m^{-3} (ave. 38.4 ng m^{-3}) during daytime and 4.96-354

ng m^{-3} (66.0 ng m^{-3}) during nighttime (Tables 1 and S1, Figure 5a), although the values

are lower than previous results reported in Nanjing (Wang and Kawamura, 2005).

Levoglucosan could account for up to 90% of total sugars in Chinese urban

aerosols (Wang et al., 2006). The contribution of levoglucosan to OC and WSOC were

0.02-0.51% (ave. 0.09%) and 0.03-0.57% (0.13%) in daytime and 0.02-0.48% (0.13%)

and 0.03-0.78% (0.22%) in nighttime, respectively. Galactosan and mannosan were also

detected in the aerosol samples. The amounts of galactosan were found to be 0.65-7.47

ng m^{-3} (ave. 2.26 ng m^{-3}) in daytime and 0.48–7.75 ng m^{-3} (3.13 ng m^{-3}) in nighttime,

whereas those of mannosan were 0.36-4.30 ng m^{-3} (1.62 ng m^{-3}) in daytime and 0.27-

5.73 ng m^{-3} (2.06 ng m^{-3}) in nighttime (Table S1 and Figure 5a). Levoglucosan showed

similar temporal trends and strong correlations with galactosan (r = 0.87, p<0.001) and

mannosan (r = 0.84, p<0.001) (Figure S2a). It should be noted that the levoglucosan

level in this study is 4-6 times lower than that of a previous study in Nanjing (Table 2)

(Wang and Kawamura, 2005). This result implies that biomass-burning emissions have

been decreased significantly in the last decade in the Nanjing area during winter.

We detected four lignin and resin products, i.e., 4-hydroxybenzoic, vanillic,

syringic, and dehydroabietic acids, which have been used as biomass-burning tracers

(Simoneit et al., 2004c). Lignin is a wood polymer, which can produce phenolic acids

during burning whereas dehydroabietic acid is more specific to conifer resin (Simoneit,

2002). We found that 4-hydroxybenzoic acid was dominant among all lignin and resin

products identified in Nanjing samples (Figure 5b). The concentration ranges of 4-

hydroxybenzoic, vanillic and syringic acids in day- and night-time were 0.65-4.31 ng m^{-}

^{3} (ave. 1.80 ng m^{-3}) and 0.62-4.96 ng m^{-3} (2.01 ng m^{-3}), 0.04-0.92 ng m^{-3} (0.25 ng m^{-3})

377   and 0.08-0.66 ng m^{-3} (0.25 ng m^{-3}), and 0.04-0.57 ng m^{-3}(0.17 ng m^{-3}) and 0.05-0.43 ng

378   m^{-3} (0.20 ng m^{-3}), respectively. The value of dehydroabietic acid was observed 0.11-

379   1.16 ng m^{-3} (0.46 ng m^{-3}) during daytime and 0.00-8.29 ng m^{-3} (0.93 ng m^{-3}) during

380   nighttime. The levels of lignin and resin acids in this study are 1-10 orders of magnitude

381   lower than those from India (Fu et al., 2010) and China (Wang et al., 2006). Lignin

382   products showed strong correlations with levoglucosan (r = 0.60-0.72, p<0.001),

383   suggesting the similar sources and origins. In contrast, there is no correlation of

384   dehydroabietic acid with levoglucosan (r = 0.07), indicating a different source of

385   dehydroabietic acid in Nanjing aerosols. The low concentrations of dehydroabietic acid

386   imply that boreal conifer forest fires are not important for the Nanjing aerosols.

387   **3.3.3 Primary sugars and sugar alcohols**

388   Sugar compounds are considered as tracers for primary biological aerosol

389   particles, which are water-soluble and thus contribute to WSOC in aerosol particles

390   (Elbert et al., 2007; Medeiros et al., 2006; Yttri et al., 2007). Four primary sugars

391   (glucose, fructose, trehalose, and sucrose) and four sugar alcohols (erythritol, arabitol,

392   mannitol, and inositol) were identified in the aerosol samples from Nanjing. The sugar

393   compounds are generated from micro-organism (pollen, fungi, and bacteria), plants,

394   flowers, resuspension of surface soil and unpaved road dust (Graham et al., 2003;

395   Simoneit et al., 2004a; Yttri et al., 2007). They can also be originated during biomass

396   burning. Total concentrations of primary sugars measured were 0.78-7.02 ng m^{-3} (ave.

397   2.90 ng m^{-3}) in daytime and 0.50-6.58 ng m^{-3} (2.98 ng m^{-3}) in nighttime, whereas those

398   of sugar alcohols were 0.30-2.90 ng m^{-3} (1.16 ng m^{-3}) during daytime and 0.19-2.75 ng

399   m^{-3} (1.27 ng m^{-3}) during nighttime.

400   Most primary sugars exhibited higher concentrations in daytime than nighttime

401   except for glucose (Figure 5c). Graham et al. (2003) proposed that fructose and glucose

402   along with sucrose are emitted as fern spores, pollen, and other "giant" bioaerosol

403   particles in daytime. Glucose showed a significant correlation with levoglucosan (r =

404   0.75, p<0.001) (Figure S2d), indicating that it is associated with biomass burning,

405   which can interpret high levels of glucose in nighttime, whereas other primary sugars

406   showed weak correlations with levoglucosan (r = 0.05-0.09). Biomass burning as a

407   source of glucose has also been proposed by Fu et al. (2008). Trehalose is mostly

408   derived from microorganisms such as bacteria, fungi, and yeast and also small amount

409   from higher plants, and invertebrates (Medeiros et al., 2006). It is also considered as a

410   product of unpaved road dust and resuspension of surface soil (Simoneit et al., 2004b;

411   Wang and Kawamura, 2005).

412   On the contrary, all sugar alcohols presented higher concentrations in nighttime

413   than in daytime while the scenario is opposite for primary sugars. Significant

414   correlations were observed between sugar alcohols and levoglucosan (r = 0.51-0.75,

415   p<0.001), suggesting a contribution of biomass burning to primary bio-aerosol particles,

416   which can explain their higher concentrations in nighttime. Previous articles proposed

417   that a huge amount of sugars and sugar alcohols can be emitted through the combustion

418   of green vegetation from temperate forests (Medeiros and Simoneit, 2008). The sugar

419   polyols are produced mainly from microbial sources, e.g., fungi, bacteria. They can also

420   release from the bark of trees, leaves, and branches. The values of sugar compounds in

421   this study are lower than other Chinese urban areas (Wang et al., 2006).

422   **3.3.4 Polycyclic aromatic hydrocarbons**

423   PAHs have severe health effect due to their genotoxicity and carcinogenicity.

424   These aromatic compounds are mainly emitted from anthropogenic activities, including

425   biomass burning, coal combustion, vehicular emissions, and natural gas combustion.

426   PAHs showed a weak positive correlation with levoglucosan (r = 0.20), suggesting that

there is no serious contribution of PAHs from biomass burning activities in Nanjing
aerosols. Total seventeen PAHs were identified in the Nanjing samples with the
concentration range of 29.5-106 ng m^{-3} (ave. 54.5 ng m^{-3}) in daytime and 21.7-223 ng
m^{-3} (72.5 ng m^{-3}) in nighttime (Tables 1 and S1, Figure 2). The higher concentrations of
PAHs in nighttime might be due to the lower dispersion of the boundary layer at night
(Figure 6a). Furthermore, households coal combustion has a significant contribution to
the air quality in China during winter (Kerimray et al., 2017). Temperature falls down
during nighttime resulting in the uses of a large amount of coal for house heating in a
rural area due to a cold weather. Heavy-duty trucks that are permitted by the local
government to work only at night as well as coal combustion should contribute to
higher concentrations of PAHs into the air in nighttime. Our values are 3-4 times higher
than those found in Hong Kong (14 ng m^{-3}) but lower than those in Beijing winter
aerosols (208 ng m^{-3}) (Wang et al., 2006). Fluoranthene was found as a dominant PAH
(ave. 8.24 ng m^{-3}) in Nanjing aerosol samples followed by chrysene (6.72 ng m^{-3}),
pyrene (6.42 ng m^{-3}) and benzo(b)fluoranthene (BbF) (5.85 ng m^{-3}) (Figure 6a).

PAHs can be further photooxidized to form SOA, i.e., phthalic acid in the
atmosphere (Zhang et al., 2016). Ding et al. (2007) proposed that PAHs could be
degraded during long-range transport. Therefore, the ratios of PAH isomer pairs can be
used to interpret the chemical aging of PAHs in the atmosphere. Benzo[a]anthracene
(BaA) and benzo(a)pyrene (BaP) are expected to be degraded more easily than their
isomers during transportation due to their higher reactivity. Thus, the lower ratios (<1.0)
of benzo[a]anthracene (BaA)/chrysene (Chry) and benzo(a)pyrene (BaP)/
benzo(e)pyrene (BeP) indicate relatively more photochemical processing of PAHs. The
ratios of BaA/Chry and BaP/BeP were calculated 0.79 and 0.88, respectively, which

451 imply that PAHs of Nanjing aerosols were more aged due to the atmospheric

452 transportation from long distances.

453   Characteristic ratios of PAHs are indicative of their specific sources. Previous

454 studies (Wang et al., 2007a, 2009; Bi et al., 2005) pointed out that the concentration

455 ratios of indeno(1,2,3-cd)pyrene to benzo(ghi)perylene (IP/BghiP), and

456 benzo(ghi)perylene to benz(e)pyrene (BghiP/BeP), are indicative of different emission

457 sources (Table 3). The ratios of IP/BghiP nearby 0.22, 0.50 and 1.3 are attributable to

458 gasoline, diesel, and coal combustion sources, respectively. On the other hand,

459 BghiP/BeP ratio of 2.0 indicates mobile exhausts and 0.8 indicates coal combustion

460 emissions (Grimmer et al., 1983; Ohura et al., 2004). Furthermore, the

461 fluoranthene/(fluoranthene+pyrene) (Flut/(Flut + Pyr)) ratios of 0.46-0.56 indicate

462 vehicular emissions, especially from catalytic converter-equipped automobiles (0.44),

463 whereas IP/(BghiP+IP) ratios (0.18, 0.37 and 0.56) are for cars, diesel, and coal

464 combustion, respectively (Bi et al., 2005).

465   In this study, we found the ratios of IP/BghiP, Bghi/Bep, Flut/(Flut + Pyr), and

466 IP/(IP+BghiP) are 1.23, 1.17, 0.56, and 0.55, respectively. The ratios are closer to those

467 in coal burning emissions than in vehicular exhausts. These results imply that PAH

468 components in Nanjing winter aerosols are mainly derived from coal combustion. The

469 PAH compositions of our study are different from those reported from Sacramento

470 (Kleeman et al., 2008), Los Angeles and London (Finlayson-Pitts and Pitts Jr, 2000), in

471 which BghiP/BeP ratios are 5.6, 3.5 and 1.7, respectively, when vehicular emissions

472 were the major sources for PAHs in these cities. The present PAH concentrations in

473 Nanjing aerosols are lower than those found in a previous study from Nanjing samples

474 collected in 2004 (Table 2) (Wang et al., 2007a) and one-fourth of those collected in

475   2001 (214 ng m^{-3}) (Yang et al., 2005), indicating the local air quality in Nanjing is

476   improving since 2001.

477   **3.3.5 Hopanes and Steranes**

478   Hopane and sterane isomers are considered as biomarkers of fossil fuel

479   emissions, which belong to the higher boiling fraction of crude oil and are more

480   resistant to degradation than *n*-alkanes. They are abundantly originated from the crude

481   oil and engine oil, and consequently in vehicle exhaust from unburned lubricating oil

482   residues and road dust (Ding et al., 2009). Six hopane compounds were identified in the

483   Nanjing urban samples (Table S1) with higher levels in nighttime (0.13-26.1 ng m^{-3},

484   ave. 4.16 ng m^{-3}) and lower levels in daytime (0.09-20.8 ng m^{-3}, 3.78 ng m^{-3}) (Figure 2).

485   The concentrations of hopane in the present study are comparable with those from other

486   Chinese cities and Tokyo (0.7-15 ng m^{-3}; 5.5 ng m^{-3}) (Wang et al., 2006). Wang et al.

487   (2009) reported that concentrations of hopanes in the urban samples were 2 orders of

488   magnitude higher than those in the mountain samples whereas hopanes were not

489   detectable in the marine samples.

490   The diagnostic ratios of hopanes can differentiate their sources (Table 3). The

491   17α(H)-21β(H)-29-norhopane (C$_{29}\alpha\beta$)/17α(H)-21β(H)-hopane (C$_{30}\alpha\beta$) ratios of 0.59-

492   0.66, 0.42, and 0.58-2.0 are attributable to gasoline, diesel and coal burning emissions,

493   respectively (Rogge et al., 1993a; Oros and Simoneit, 2000). In addition, the ratios of

494   17α(H)-21β(H)-22S-homohopane/(17α(H)-21β(H)-22S-homohopane + 17α(H)-21β(H)-

495   22R-homohopane) [C$_{31}\alpha\beta$S/(C$_{31}\alpha\beta$S + C$_{31}\alpha\beta$R)] ranging from 0.60-0.62, 0.50, and

496   0.05-0.37 indicate gasoline, diesel and coal burning emissions, respectively (Rogge et

497   al., 1993a; Oros and Simoneit, 2000). We observed that concentration ratios of

498   C$_{29}\alpha\beta$/C$_{30}\alpha\beta$ and C$_{31}\alpha\beta$S/(C$_{31}\alpha\beta$S+ C$_{31}\alpha\beta$R) in this study are 0.58 and 0.48,

499   respectively, which are near to those in vehicular emissions than coal combustion. Thus,

500 hopanes in the Nanjing aerosol are predominantly emitted from traffic emissions due to

501 rapidly increasing of automobiles in Chinese mega-cities.

502   A series of steranes were also identified in the present study. Concentration

503 ranges of total steranes were 1.14-9.16 ng m^{-3} (ave. 2.29 ng m^{-3}) during daytime and

504 1.09-11.1 ng m^{-3} (2.64 ng m^{-3}) during nighttime. The diurnal distribution patterns of

505 steranes showed remarkable similarity with hopanes. The strong correlation coefficient

506 was also observed between steranes and hopanes (r = 0.94, p<0.001), indicating their

507 similar emission sources (Figure S3d). It is reasonable because homologues of hopanes

508 and steranes are very stable and have similar atmospheric fates (Ding et al., 2009). In

509 contrast, PAHs showed positive correlations with hopanes and steranes with a lower

510 correlation coefficient (r = 0.42, p<0.001), indicating their partly similar sources.

511 **3.3.6 Phthalates**

512   Phthalates are common additives widely used as a softener and plasticizers in

513 polyvinylchloride (PVC) and synthetic polymers, respectively. It can be emitted into the

514 atmosphere through the evaporation process due to their weak bonding in the polymer.

515 Phthalates have potential health effect due to their endocrine disrupting and

516 carcinogenic properties (Sidhu et al., 2005). It is necessary to pay attention to phthalates

517 as toxic components in the aerosol particles. However, few studies have reported their

518 atmospheric distribution over China (Fu et al., 2008; Wang et al., 2006, 2007a). Four

519 phthalate esters, i.e., diethyl (DEP), di-iso-butyl (DiBP), di-n-butyl (DnBP), and di-(2-

520 ethylhexyl) (DEHP) phthalates were characterized in this study with total

521 concentrations of 13.9 ng m^{-3} (range, 2.66-40.0 ng m^{-3}) in daytime and 16.3 ng m^{-3}

522 (3.79-51.8 ng m^{-3}) in nighttime (Figure 7a). DnBP (ave. 8.07 ng m^{-3}) is the dominant

523 tracer, followed by DEHP (4.00 ng m^{-3}), DiBP (2.59 ng m^{-3}) and DEP (0.14 ng m^{-3}).

524 The levels of phthalates in this study are 4-20 times lower than those proposed in other

Chinese megacities in 2006 (Wang et al., 2006), although comparable than those observed from Paris, France (8.2 ng m^{-3}) (Teil et al., 2006), Sweden (3.7 ng m^{-3}) (Thuren and Larsson, 1990), and Texas, USA (2.1 ng m^{-3}) (Weschler, 1984).

The evaporation of phthalates can be accelerated under high ambient temperature conditions. The higher values in nighttime than daytime of phthalates in Nanjing aerosol is opposite with the result of Mt. Tai aerosols (Fu et al., 2008) due to the decreased PBLH in nighttime. Moreover, there is no significant difference in temperature between day and night during the campaign in Nanjing (Figure S1). Significant correlations were found between DEP and DiBP (r = 0.85, p<0.001) as well as DiBP and DnBP (r = 0.87, p<0.001) (Figures S4a and S4b), suggesting that these compounds are commonly used as plasticizers in China and released in the same way into the atmosphere. It should be noted that the concentration level of phthalates in this study is 1-2 orders of magnitude lower than those found in Nanjing aerosols collected in 2004 (ave. 230 ng m^{-3}) (Wang et al., 2007a), suggesting a significant improvement of local air quality in Nanjing regarding plastic emission.

3.3.7 Aromatic acids

We detected benzoic acid and three phthalic acids in the urban aerosols from Nanjing with total concentrations of 6.70 ng m^{-3} (1.53-23.1 ng m^{-3}) in daytime and 8.37 ng m^{-3} (1.99-18.5 ng m^{-3}) in nighttime (Figure 7b). These acids can play a significant role to increase the formation of new particles in the atmosphere (Zhang et al., 2004). Benzoic acid ranged from 0.17-0.95 ng m^{-3} (ave. 0.45 ng m^{-3}) in daytime and 0.24-1.22 ng m^{-3} (0.54 ng m^{-3}) in nighttime (Table S1), which is 1 and 4 orders of magnitude lower than summertime aerosol of Mt. Tai and wintertime aerosol of tropical India, respectively (Fu et al., 2008, 2010). Benzoic acid is primarily emitted from automobiles

549 (Rogge et al., 1993b; Kawamura et al., 2000) but also been proposed as a secondary

550 component via a photooxidation of several aromatic hydrocarbons (Fu et al., 2010).

551   Total phthalic acids varied from 1.40-21.9 ng m^{-3} (ave. 6.25 ng m^{-3}) during

552 daytime and 1.76-16.8 ng m^{-3} (7.83 ng m^{-3}) during nighttime. Their concentrations are

553 lower than those found during aircraft measurement over China in summer (17±13 ng

554 m^{-3}) (Wang et al., 2007b) but higher than the samples measured from the northwestern

555 Pacific (ave. 1.5 ng m^{-3}) (Simoneit et al., 2004a). The molecular distributions of

556 phthalic acids showed the dominance of terephthalic acid (Figure 7b), which accounted

557 for 82% of total aromatic acids in Nanjing samples. Phthalic acids are SOA products

558 produced from several PAHs (Oliveira et al., 2007; Fine etal., 2004). It is noteworthy

559 that PAHs mostly produce phthalic acids over the North China Plain (Fu et al., 2008).

560 Terephthalic acid can be derived from plastics burning as well (Fu et al., 2010).

561   Aromatic acids showed positive correlations with 4 and 5 rings PAHs (r = 0.56,

562 p<0.001) and phthalates (r = 0.71, p<0.001) (Figure S3c), suggesting that they are

563 primarily derived from PAHs. Furthermore, aromatic acids showed significant

564 correlation with oxidation products of polyacids (r = 0.83, p<0.001) (Figure S4c),

565 indicating the secondary oxidation process is a major source of aromatic acids.

566 However, higher concentrations of aromatic acids in nighttime rather than daytime may

567 not explain photochemical oxidation. We propose two explanations for the high level of

568 SOA products in nighttime. First, SOA products are formed during long-range

569 atmospheric transport that is consistent with aged PAHs in the aerosols as discussed

570 above (section 3.3.4). Second, NOx can play an important role to oxidize PAHs in

571 nighttime when NOx concentration is high (Offenberg et al., 2007; Henze et al., 2008).

572 However, further studies are needed for the justification of NOx influence in the

573 Nanjing atmosphere.

3.3.8 Hydroxy-/polyacids

Glycerol and several polyacids were identified in all the samples from Nanjing (Table S1). Glycerol is a primary product of a metabolic reaction of soil organisms, while polyacids are secondarily produced by photo-oxidation of organic precursors (Simoneit et al., 2004c). Glycerol didn't show significant correlation with polyacids ($r = 0.21$-0.38), implying their different sources (i.e., primary and secondary). Kawamura and Ikushima(1993), and Matsunaga et al. (1999) reported that malic acid is a photooxidation product of succinic acid, which is one of the photooxidation products of biogenic unsaturated fatty acids (BUFAs) in the atmosphere. Moreover, SOA tracers, including malic and tartaric acids are produced by the photochemical oxidation of isoprene (Claeys et al., 2004).

The concentration range of glycerol was 0.66-5.99 ng m^{-3} (ave. 2.67 ng m^{-3}) during daytime and 0.73-8.72 ng m^{-3} (3.50 ng m^{-3}) during nighttime. Glycerol is a dominant component in this group (Table S1 and Figure7c), which is consistent with the previous report from Nanjing aerosol in 2004-2005, whereas present concentration level is lower than that reported in Nanjing (Wang and Kawamura, 2005). Concentrations ranges of total polyacids were 1.21-23.5 ng m^{-3} (5.1 ng m^{-3}) during daytime and 2.05-11.2 ng m^{-3} (5.80 ng m^{-3}) during nighttime, among which tartaric acid (2.18 ng m^{-3}) was dominant (Figure 7c). Tartaric acid presented a positive correlation with levoglucosan ($r = 0.75$, $p<0.001$) (Figure S2b), suggesting an influence of biomass burning. Significant correlations were found among all polyacids ($r = 0.50$-0.75, $p<0.001$), indicating their similar source or formation pathway. Polyacids showed a strong correlation with WSOC ($r = 0.85$, $p<0.001$) (Figure S4d), indicating their water-soluble and hygroscopic nature and therefore it might influence the CCN activities of aerosol particles. It should be noted that secondary oxidation products are formed

599   during long-range atmospheric transport, which can explain high values of polyacids in

600   nighttime. This result is consistent with the high WSOC/OC ratio in Nanjing aerosols

601   (see section 3.2) as well as air mass back trajectories (Figure S5).

3.4 Source apportionment of organic aerosols using PMF

603   Positive matrix factorization (PMF5.0, USEPA) analysis was performed in this

604   study for better understanding the sources of the identified components. It is a statistical

605   source apportionment model widely used to verify underlying covariance among

606   chemical parameters (Paatero and Tapper, 1994; Jaeckels et al., 2007). Detailed

607   information of the PMF model can be found elsewhere (Paatero, 1997; Paatero and

608   Tapper, 1994). PMF model was applied for apportioning ambient PM to motor vehicle

609   and wood combustion emission, SOA, and two-point sources using organic molecular

610   markers (Jaeckels et al., 2007). This model has also been extensively used for

611   identifying source profile and source contribution of PM based elemental and organic

612   markers data (Song et al., 2001; Buzcu et al., 2003; Jaeckels et al., 2007; Jia et al.,

613   2010). The analytical errors estimated for the measured values of chemical species in

614   PMF analysis are 10%. The detected organic compound classes were subjected to

615   source apportionment evaluation to make the classifications of sources using the model.

616   PMF model application resolved 5 source factors based on Q values that contributed to

617   ambient $PM_{2.5}$ in this study. OC, EC and some inorganic ions were also used to

618   investigate possible different sources. We used $PM_{2.5}$ as the sum of total variables

619   during the model convergence. Figure 8 shows composition source profiles for the five

620   factors resolved by PMF analysis, where factor 3 is a dominant source.

621   Factor 1 is dominated by levoglucosan (69%) followed by fatty alcohol (C_{30})

622   (56%), arabitol (44%) and n-alkane (C_{29}) (34%). Factor 1 is associated with biomass

623   burning because levoglucosan is a specific tracer of biomass burning. Moreover, fatty

alcohols, fatty acids, *n*-alkanes, and sugar compounds can also be emitted from biomass burning. Biomass materials, including rice and wheat straws, and cotton stems, are widely used for domestic cooking in rural areas around Nanjing, particularly in the evening. Therefore, particles from biomass burning are abundantly released into the atmosphere and then transported to the Nanjing urban area. This idea is consistent with high loadings of biomass burning tracers during nighttime.

Factor 2 is enriched with nss-Ca^{2+} (75 %), suggesting that the component is associated with soil dust because it is a specific tracer of soil dust (Athanasopoulou et al., 2010; Brahney et al., 2013). Many infrastructures of the urban area are constructing in China, which can produce dust particles largely and emit into the atmosphere. Factor 3 is attributed to secondary oxidation products because of the dominant species in this source profile is malic acid (69%). Malic acid is a secondary oxidation product as described above (see section 3.3.8).

Factor 4 was abundantly loaded by fluoranthene (representative PAH) (79%), $C_{30}\alpha\beta$ (representative hopane) (64%) and C_{29} (representative *n*-alkane) (50%), implying their origination from the fossil fuel combustion. It should be noted that *n*-alkanes also showed a loading in factor 1, suggesting that *n*-alkanes are partly associated with biomass burning. PAHs can be emitted from fossil fuel combustion and biomass burning activities. However, we observed that PAHs are mainly derived from fossil fuel combustion in Nanjing (see section 3.3.4). Furthermore, *n*-alkanes can be originated from fossil fuel combustion and higher plant waxes, whereas fossil fuel was the dominant source for *n*-alkanes in Nanjing aerosols (see section 3.3.1). Hopanes are emitted from the vehicular exhaust as well as coal burning. Low-quality coals are extensively used in urban and rural areas in China for cooking and house heating. Many power plants in Chinese cities also used a large amount of coal for producing energy.

649 Running vehicles have also increased severely in China, which can emit hopanes in the

650 atmosphere. Factor 5 is dominated by di-(2-ethylhexyl) phthalate (DEHP) (63%)

651 followed by terephthalic acid (35%), which should be associated with plastic burning.

652 Terephthalic acid is a secondary oxidation product and also can be emitted from the

653 open burning of plastics as discussed above.

654   PMF results can be further utilized to calculate the relative contributions of

655 sources to the amount of ambient OC or $PM_{2.5}$ using a multiple linear regression

656 between the isolated factor strengths and measured OC or $PM_{2.5}$ (Song et al., 2001).

657 Results of this analysis are presented in Figure 9 whereas source contributions were

658 calculated to $PM_{2.5}$. Fossil fuel combustion was the dominant source (28.7%)

659 considering the primary source, followed by emissions of biomass burning (17.1%), soil

660 dust (14.5%), and plastic burning (6.83%) during this study period. However, secondary

661 oxidation products showed the highest contribution (32.9%) to $PM_{2.5}$ in Nanjing

662 probably due to long-range atmospheric transport. These results indicate that fossil fuel

663 combustion is an important contributor to Nanjing aerosol during winter. Wang and

664 Kawamura (2005) reported that fossil fuel combustion (52%) was the largest

665 contributor to total organics followed by biomass burning (14%) and SOA (10%) from

666 Nanjing, whereas coal combustion was found to contribute to $PM_{2.1}$ by 39.5% in 2010

667 in Nanjing (Chen et al., 2015). Gao et al. (2013) pointed out that coal combustion was

668 the dominant (58%) contributor to $PM_{2.5}$ followed by biomass burning (31%), and

669 vehicular emissions (11%) in the Pearl River Delta region (two urban, two suburban

670 and two rural sites) while sample was collected in 2009. The comparison of current

671 results with previous studies implies that the contribution of fossil fuel combustion and

672 biomass burning emission in China decreased significantly in the past decade.

However, pollution levels in China are still severe compared to those in the National and WHO standards as discussed above (section 1).

4. Summary and Conclusions

We collected PM$_{2.5}$ aerosol samples during winter from Nanjing, an urban area located in east China in 2014 to 2015. Twelve organic compound classes were identified in the aerosol samples with *n*-alkanes as the dominant compound class, followed by fatty acids, PAHs, anhydro-sugars, fatty alcohols, and phthalate esters. The concentrations of organic compounds were slightly higher at night samples than day samples because of the lower PBLH and more emissions from heavy-duty trucks as well as coal and biomass burning in nighttime.

The molecular signature of *n*-alkanes with a weak odd-carbon number predominance and maxima of C$_{29}$ (ave. CPI: 1.18) implies their significant emission from fossil fuels combustion. On the contrary, microbial and plant waxes are the major source of fatty acids and fatty alcohols in this study. Fatty alcohols are also significantly emitted from biomass burning. The biomass burning tracer, levoglucosan was the dominant species among the detected compounds. Levoglucosan and other biomass burning tracers are mainly originated from house cooking and heating during study period. Concentrations of secondary oxidation products, including aromatic acids and polyacids, maximized during nighttime possibly because of the influence of NO$_x$ or long-range atmospheric transport.

The diagnostic ratios of the tracer compounds suggest that coal burning is the major source of PAHs while hopanes are abundantly emitted from traffic emissions over Nanjing atmosphere. PMF analysis demonstrated that fossil fuel combustion is an important source (28.7%) in Nanjing winter aerosols. The concentrations of organic tracers in this study are lower than previously reported Nanjing aerosols collected in

698   2004-2005. Air quality in Nanjing may have been improved for last decade. However,

699   fossil fuel combustion emissions have not been decreased ==satisfactorily== and still control

700   the compositions of wintertime OAs in Nanjing atmosphere.

701

702   **Acknowledgements**

703   We acknowledge the Natural Scientific Foundation of China (Grant No. 91643109 and

704   41603104) and Japan Society for the Promotion of Science (Grant No. 24221001) for

705   financial support.

706

707   **References**

708   Albrecht, B. A.: Aerosols, Cloud Microphysics, and Fractional Cloudiness, Science,
709   245(4923), 1227–1230. https://doi.org/10.1126/science.245.4923.1227, 1989.
710   Asa-Awuku, A., Moore, R. H., Nenes, A., Bahreini, R., Holloway, J. S., Brock, C. A.,
711   Middlebrook, A. M., Ryerson, T. B., Jimenez, J. L., Decarlo, P. F., Hecobian, A.,
712   Weber, R. J., Stickel, R., Tanner, D. J., and Huey, L. G.: Airborne cloud
713   condensation nuclei measurements during the 2006 Texas Air Quality Study, J.
714   Geophys. Res.- Atmos., 116(11), doi:10.1029/2010JD014874, 2011.
715   Athanasopoulou, E., Tombrou, M.,Russell, A. G.. Karanasiou, A., Eleftheriadis, K., and
716   Dandou, A.: Implementation of road and soil dust emission parameterizations in the
717   aerosol model CAMx: Applications over the greater Athens urban area affected by
718   natural sources, J. Geophys. Res., 115(D17301), doi:10.1029/2009JD013207., 2010.
719   Bi, X., Sheng, G., Peng, P., Chen, Y., Zhang, Z., and Fu, J.: Distribution of particulate-
720   and vapor-phase n-alkanes and polycyclic aromatic hydrocarbons in urban
721   atmosphere of Guangzhou, China, Atmos. Environ., 37(2), 289–298, 2003.
722   Bi, X., Sheng, G., Peng, P., Chen, Y., and Fu, J.: Size distribution of n-alkanes and
723   polycyclic aromatic hydrocarbons (PAHs) in urban and rural atmospheres of
724   Guangzhou, China, Atmos. Environ., 39(3), 477–487,, 2005.
725   Boreddy, S. K. R., Haque, M. M., and Kawamura, K.: Long-term (2001-2012) trends of
726   carbonaceous aerosols from a remote island in the western North Pacific: An outflow
727   region of Asian pollutants, Atmos. Chem. Phys., 18(2), 1291–1306, doi:10.5194/acp-
728   18-1291-2018, 2018.
729   Brahney, J., Ballantyne, A. P., Sievers, C., and Neff, J. C.: Increasing Ca^{2+} deposition
730   in the western US: The role of mineral aerosols, Aeolian Res., 10, 77–87, 2013.
731   Buzcu, B., Fraser, M. P., Kulkarni, P., and Chellam, S.: Source identification and
732   apportionment of fine particulate matter in Houston, TX, using positive matrix
733   factorization, Environ. Eng. Sci., 20(6), 533–545, 2003.
734   ==Chang, Y., Zhang, Y., Tian, C., Zhang, S., Ma, X., Cao, F., Liu, X., Zhang, W., Kuhn,==
735   ==T., and Lehmann, M. F.: Nitrogen isotope fractionation during gas-particle==
736   ==conversion of NOx to NO_3^- in the atmosphere – implications for isotope-based NOx==
737   ==source apportionment, Atmos. Chem. Phys., 18, 11647-11661, https:// doi.org/==
738   ==10.5194/acp-18-11647-2018, 2018.==

739 Chen, P., Wang, T., Hu, X., and Xie, M: Chemical Mass Balance Source
740   Apportionment of Size-Fractionated Particulate Matter in Nanjing, China, Aerosol
741   and Air Quality Research, 15, 1855–1867, 2015.
742 Chung, S. H., and Seinfeld, J. H.: Global distribution and climate forcing of
743   carbonaceous aerosols, J. Geophys. Res.- Atmos., 107((D19)), 4407,
744   doi:10.1029/2001JD001397, 2002.
745 Chung, C. E., Ramanathanb, V., and Decremer, D.: Observationally constrained
746   estimates of carbonaceous aerosol radiative forcing, PNAS, 109, 11624–11629; 109,
747   11624–11629, doi:10.1073/pnas.1203707109, 2012.
748 Claeys, M., Graham, B., Vas, G., Wang, W., Vermeylen, R., Pashynska, V., Cafmeyer,
749   J., Guyon, P., Andreae, M. O., Artaxo, P., and Maenhaut, W.: Formation of
750   secondary organic aerosols through photooxidation of isoprene, Science (80-.).,
751   303(5661), 1173–1176, 2004.
752 Cooke, W. F., Liousse, C., Cachier, H., and Feichter, J.: Construction of a 1 degrees x 1
753   degrees fossil fuel emission data set for carbonaceous aerosol and implementation
754   and radiative impact in the ECHAM4 model, J. Geophys. Res.- Atmos., 104(D18),
755   22137–22162, 1999.
756 Ding, X., Wang, X. M.,Xie, Z. Q., Xiang, C. H., Mai, B. X., Sun, L. G., Zheng, M.,
757   Sheng, G. Y., Fu, J. M., and Pöschl, U.: Atmospheric polycyclic aromatic
758   hydrocarbons observed over the North Pacific Ocean and the Arctic area: Spatial
759   distribution and source identification, Atmos. Environ., 41, 2061–2072, 2007.
760 Ding, L. C., Fu, K.,Wang, D. K. W.,Dann, T., andAustin, C. C.: A new direct thermal
761   desorption-GC/MS method: Organic speciation of ambient particulate matter
762   collected in Golden, BC, Atmos. Environ., 43, 4894–4902, 2009.
763 Ding, X., Wang, X., Xie, Z., Zhang, Z., and Sun, L.: Impacts of siberian biomass
764   burning on organic aerosols over the north pacific ocean and the arctic: Primary and
765   secondary organic tracers, Environ. Sci. Technol., 47(7), 3149–3157, 2013.
766 Dusek, U., Frank, G. P., Hildebrandt, L., Curtius, J., Schneider, J., Walter, S., Chand,
767   D., Drewnick, F., Hings, S., Jung, D., Borrmann, S., and Andreae, M. O.: Size
768   matters more than chemistry for cloud-nucleating ability of aerosol particles, Science
769   (80-.)., 312(5778), 1375–1378, 2006.
770 Elbert, W., Taylor, P. E., Andreae, M. O., and Poschl, U.: Contribution of fungi to
771   primary biogenic aerosols in the atmosphere: wet and dry discharged spores,
772   carbohydrates, and inorganic ions, Atmos. Chem. Phys., 7, 4569–4588, 2007.
773 Finlayson-Pitts, B. J., and Pitts Jr, J. N.: Chemistry of the Upper and Lower
774   Atmosphere, Academic Press, San Diego, 2000.
775 Fine, P. M., Chakrabarti, B., Krudysz, M., Schauer, J. J., and Sioutas, C.: Diurnal
776   variations of individual organic compound constituents of ultrafine and accumulation
777   mode particulate matter in the Los Angeles basin, Environ. Sci. Technol., 38(5),
778   1296–1304, 2004.
779 Fu, P. Q., Kawamura, K., Okuzawa, K., Aggarwal, S. G., Wang, G., Kanaya, Y., and
780   Wang, Z.: Organic molecular compositions and temporal variations of summertime
781   mountain aerosols over Mt. Tai, North China Plain, J. Geophys. Res.-Atmos., 113,
782   D1910, doi:10.1029/2008JD009900, 2008.
783 Fu, P. Q., Kawamura, K., and Barrie, L. A.: Photochemical and other sources of organic
784   compounds in the Canadian high Arctic aerosol pollution during winter-spring,
785   Environ. Sci. Technol., 43(2), 286–292, 2009.
786 Fu, P. Q., Kawamura, K., Pavuluri, C. M., Swaminathan, T., and Chen, J.: Molecular
787   characterization of urban organic aerosol in tropical India: contributions of primary
788   emissions and secondary photooxidation, Atmos. Chem. Phys., 10(6), 2663–2689,
789   2010.
790 Gao, B., Guo, H., Wang, X. M., Zhao, X. Y., Ling, Z. H., and Zhang, Z.: Tracer-based

source apportionment of polycyclic aromatic hydrocarbons in PM$_{2.5}$ in Guangzhou southern China, using positive matrix factorization (PMF). Environ. Sci. Poll. Res. Int., 20, 2398–2409, 2013.

Graham, B., Guyon, P., Taylor, P. E., Artaxo, P., Maenhaut, W., Glovsky, M. M., Flagan, R. C., and Andreae, M. O.: Organic compounds present in the natural Amazonian aerosol: Characterization by gas chromatography-mass spectrometry, J. Geophys. Res.-Atmos., 108, D24, 4766, doi:10.1029/2003JD003990, 2003.

Grimmer, G., Jacob, J., and Noujack, K. W.: Profile of the polycyclic aromatic hydrocarbons from lubricating oils. Inventory by GC/MS-PAH in environmental materials, part 1., Fresenius Zeitschrift fur Anal. Chemie, 314, 13–19., 1983.

Guo, Z. G., Sheng, L. F., Feng, J. L., and Fang, M.: Seasonal variation of solvent extractable organic compounds in the aerosols in Qingdao, China, Atmos. Environ., 37(13), 1825–1834, doi:10.1016/S1352-2310(03)00064-5, 2003.

Haque, M. M., Kawamura, K., and Kim, Y.: Seasonal variations of biogenic secondary organic aerosol tracers in ambient aerosols from Alaska, Atmos. Environ., 130, 95–104, doi:10.1016/j.atmosenv.2015.09.075, 2016.

Hays, M. D., Fine, P. M., Geron, C. D., Kleeman, M. J., and Gullett, B. K.: Open burning of agricultural biomass: Physical and chemical properties of particle-phase emissions, Atmos. Environ., 39(36), 6747–6764, 2005.

He, K., Zhao, Q., Ma, Y., Duan, F., Yang, F., Shi, Z., and Chen, G: Spatial and seasonal variability of PM$_{2.5}$ acidity at two Chinese megacities: insights into the formation of secondary inorganic aerosols, Atmos. Chem. Phys., 12, 1377–1395, doi:10.5194/acp-12-1377-2012, 2012.

Henze, D. K., Seinfeld, J. H., Ng, N. L., Kroll, J. H., Fu, T. M., Jacob, D. J., and Heald, C. L.: Global modeling of secondary organic aerosol formation from aromatic hydrocarbons: high- vs. low-yield pathways, Atmos. Chem. Phys., 8(9), 2405–2420, doi:10.5194/acp-8-2405-2008, 2008.

Huebert, B. J., Bates, T., Russell, P. B., Shi, G. Y., Kim, Y. J., Kawamura, K., Carmichael, G., and Nakajima, T.: An overview of ACE-Asia: Strategies for quantifying the relationships between Asian aerosols and their climatic impacts, J. Geophys. Res.-Atmos., 108(D23), doi:10.1029/2003JD003550, 2003.

Jacobson, M. Z.: Global direct radiative forcing due to multicomponent anthropogenic and natural aerosols, J. Geophys. Res.- Atmos., 106(D2), 1551–1568, doi:10.1029/2000JD900514, 2001.

Jaeckels, J. M., Bae, M. S., and Schauer, J. J.: Positive matrix factorization (PMF) analysis of molecular marker measurements to quantify the sources of organic aerosols, Environ. Sci. Technol., 41(16), 5763–5769, 2007.

Jia, Y. L., Clements, A. L., and Fraser, M. P.: Saccharide composition in atmospheric particulate matter in the southwest US and estimates of source contributions, J. Aerosol Sci., 41(1), 62–73, doi:10.1016/j.jaerosci.2009.08.005, 2010.

Kanakidou, M., Seinfeld, J. H., Pandis, S. N., Barnes, I., Dentener, F. J., Facchini, M. C., Van Dingenen, R., Ervens, B., Nenes, A., Nielsen, C. J., Swietlicki, E., Putaud, J. P., Balkanski, Y., Fuzzi, S., Horth, J., Moortgat, G. K., Winterhalter, R., Myhre, C. E. L., Tsigaridis, K., Vignati, E., Stephanou, E. G., and Wilson, J.: Organic aerosol and global climate modelling: a review, Atmos. Chem. Phys., 5, 1053–1123, 2005.

Kawamura, K., and Gagosian, R. B.: Implications of ω-oxocarboxylic acids in the remote marine atmosphere for photo-oxidation of unsaturated fatty acids, Nature, 325, 330–332, 1987.

Kawamura, K., and Ikushima, K.: Seasonal changes in the distribution of dicarboxylic acids in the urban atmosphere, Environ. Sci. Technol., 27(10), 2227–2235, 1993.

Kawamura, K., Kosaka, M., and Sempéré, R.: Distributions and seasonal changes of hydrocarbons in urban aerosols and rainwaters, Chikyukagaku (Geochemistry), 29, 1–15, 1995.

Kawamura, K., Steinberg, S., and Kaplan, I. R.: Homologous series of C$_1$-C$_{10}$ monocarboxylic acids and C$_1$-C$_6$ carbonyls in Los Angeles air and motor vehicle exhausts, Atmos. Environ., 34(24), 4175–4191, 2000.

Kawamura, K., Ishimura, Y., and Yamazaki, K.: Four years' observations of terrestrial

848   lipid class compounds in marine aerosols from the western North Pacific, Glob.
849   Biogeochem. Cycles,. 17, 1003(1), doi:10.1029/2001GB001810, 2003.

850 Kendrick, C. M., Koonce, P., and George, L. A.: Diurnal and seasonal variations of NO,
851   NO_2 and $PM_{2.5}$ mass as a function of traffic volumes alongside an urban arterial,
852   Atmos. Environ., 122, 133–141, doi:10.1016/j.atmosenv.2015.09.019, 2015.

853 Kerimray, A., Luis, R.-S., Torkmahalleh, M. A., Hopke, P. K., Gallachóir, B. P. Ó.:
854   Coal use for residential heating: Patterns, health implications and lessons learned,
855   Ener. Sus. Devlop., 40, 19–30, 2017.

856 Kleeman, M. J., Riddle, S. G., and Jakober, C. A.: Size distribution of particle-phase
857   molecular markers during a severe winter pollution episode, Environ. Sci. Technol.,
858   42, 6469–6475, 2008.

859 Kolattukudy, P. E.: Chemistry and Biochemistry of Natural Waxes, Elsevier, New
860   York., 1976.

861 Kunwar, B., and Kawamura, K.: One-year observations of carbonaceous and
862   nitrogenous components and major ions in the aerosols from subtropical Okinawa
863   Island, an outflow region of Asian dusts, Atmos. Chem. Phys., 14, 1819–1836,
864   doi:https://doi.org/10.5194/acp-14-1819-2014, 2014.

865 Li, M., Zhang, Q., Kurokawa, J.-I., Woo, J-H., He, K., Lu, Z., Ohara, T., Song, Y.,.
866   Streets, D. G., Carmichael, G. R., Cheng, Y., Hong, C., Huo, H., Jiang, X., Kang, S.,
867   Liu, F., Su, H., and Zheng, B: MIX: a mosaic Asian anthropogenic emission
868   inventory under the international collaboration framework of the MICS-Asia and
869   HTAP, Atmos. Chem. Phys., 17, 935–963, 2017.

870 Liu, J., Han, Y., Tang, X., Zhu, J., and Zhu, T: Estimating adult mortality attributable to
871     $PM_{2.5}$ exposure in China with assimilated $PM_{2.5}$ concentrations based on a ground
872   monitoring network. Sci. Total Environ., 568, 1253–1262. doi:10.1016/j.scitotenv.
873   2016.05.165, 2016.

874 Lohmann, U., Feichter, J., Penner, J., and Leaitch, R.: Indirect effect of sulfate and
875   carbonaceous aerosols: A mechanistic treatment, J. Geophys. Res.- Atmos.,
876   105(D10), 12193–12206, doi:10.1029/1999JD901199, 2000.

877 Matsunaga, S., Kawamura, K., Nakatsuka, T., and Ohkouchi, N.: Preliminary study on
878   laboratory photochemical formation of low molecular weight dicarboxylic acids from
879   unsaturated fatty acid (oleic acid), Res. Org. Geochem., 14, 19–25, 1999.

880 Ma, Z., Hu, X., Sayer, A. M., Levy, R., Zhang, Q., Xue, Y., Tong, S., Bi, J., Huang, L.,
881   Liu, Y.: Satellite-based spatiotemporal trends in $PM_{2.5}$ concentrations: China, 2004–
882   2013, Environ. Health Perspect., 124, 184–192, http://dx.doi.org/10.1289/
883   ehp.1409481, 2016.

884 Medeiros, P. M., Conte, M. H., Weber, J. C. and Simoneit, B. R. T.: Sugars as source
885   indicators of biogenic organic carbon in aerosols collected above the Howland
886   Experimental Forest, Maine, Atmos. Environ., 40(9), 1694–1705, 2006.

887 Medeiros, P. M., and Simoneit, B. R. T.: Source profiles of organic compounds emitted
888   upon combustion of green vegetation from temperate climate forests, Environ. Sci.
889   Technol., 42(22), 8310–8316, 2008.

890 Mochida, M., Kitamori, Y., Kawamura, K., Nojiri, Y., and Suzuki, K.: Fatty acids in the
891   marine atmosphere: Factors governing their concentrations and evaluation of organic
892   films on sea-salt particles, J. Geophys. Res.-Atmos., 107, D17, 4325,
893   doi:10.1029/2001JD001278, 2002.

894 Mochida, M., Kawamura, K., Fu, P., and Takemura, T.: Seasonal variation of
895   levoglucosan in aerosols over the western North Pacific and its assessment as a
896   biomass-burning tracer, Atmos. Environ., 44, 3511-3518, 2010.

897 Mochizuki, T., Miyazaki, Y., Ono, K., Wada, R., Takahashi, Y., Saigusa, N.,
898   Kawamura, K., and Tani, A.: Emissions of biogenic volatile organic compounds and
899   subsequent formation of secondary organic aerosols in a Larix kaempferi forest,
900   Atmos. Chem. Phys., 15(20), 12029–12041, doi:10.5194/acp-15-12029-2015, 2015.

901 O'Dowd, C. D., Facchini, M. C., Cavalli, F., Ceburnis, D., Mircea, M., Decesari, S.,

902 Fuzzi, S., Yoon, Y. J., and Putaud, J. P.: Biogenically driven organic contribution to
903 marine aerosol, Nature, 431, 676–680, 2004.
904 Offenberg, J., Lewis, C., Lewandowski, M., Jaoui, M.,Kleindienst, T. E., and Edney, E.
905 O.: Contributions of Toluene and α-Pinene to SOA formed in an irradiated toluene/α-
906 Pinene/NOx/air mixture: Comparison of results using ^{14}C content and SOA organic
907 tracer methods, Environ. Sci. Tec., 41, 3972–3976, 2007.
908 Ohura, T., Amagai, T., Fusaya, M., and Matsushita, H.: Polycyclic Aromatic
909 Hydrocarbons in Indoor and Outdoor Environments and Factors Affecting Their
910 Concentrations, Environ. Sci. Technol., 38(1), 77–83, doi:10.1021/es030512o, 2004.
911 Oliveira, C., Pio, C., Alves, C., Evtyugina, M., Santos, P., Goncalves, V., Nunes, T.,
912 Silvestre, A. J. D., Palmgren, F., Wahlin, P., and Harrad, S.: Seasonal distribution of
913 polar organic compounds in the urban atmosphere of two large cities from the North
914 and South of Europe, Atmos. Environ., 41, 5555–5570, 2007.
915 Oros, D. R., and Simoneit, B. R. T.: Identification and emission rates of molecular
916 tracers in coal smoke particulate matter, Fuel, 79(5), 515–536, doi:10.1016/S0016-
917 2361(99)00153-2, 2000.
918 Paatero, J.: Least squares formulation of robustnon-negative factor analysis., Chemom.
919 Andin., 37(1), 23–35, 1997.
920 Paatero, P., and Tapper, U.: Positive Matrix Factorization - A Nonnegative Factor
921 Model With Optimal Utilization of Error-Estimates of Data Values, Environmetrics,
922 5(2), 111–126, doi:10.1002/env.3170050203, 1994.
923 Pani, S. K., Lee, C. T., Chou, C. C. K., Shimada, K., Hatakeyama, S., Takami, A.,
924 Wang, S. H., and Lin, N. H.: Chemical Characterization of Wintertime Aerosols over
925 Islands and Mountains in East Asia: Impacts of the Continental Asian Outflow,
926 Aerosol Air Qual. Res., 17, 3006–3036, 2017.
927 Pope, C. A., Ezzati, M., and Dockery, D. W.: Fine-particulate air pollution and life
928 expectancy in the United States, N. Engl. J. Med., 360, 376–386, 2009.
929 Ram, K., Sarin,M. M., and Hegde,P.: Atmospheric abundances of primary and
930 secondary carbonaceous species at two high-altitude sites in India: Sources and
931 temporal variability, Atmos. Environ., 42, 6785-6796, 2008.
932 Ramírez, N., Cuadras, A., Rovira, E., Marc e,R.M., and Borrull, F.: Risk assessment
933 related to atmospheric polycyclic aromatic hydrocarbons in gas and particle phases
934 near industrial sites, Environ. Heal. Perspect., 119(8), 1110–1116, 2011.
935 Riipinen, I., Yli-Juuti, T., Pierce, J.R., Petaja, T., Worsnop, D.R., Kulmala, M., and
936 Donahue, N. M.: The contribution of organics to atmospheric nanoparticle growth,
937 Nat. Geosci., 5, 453–458., 2012.
938 Rogge, W. F., Mazurek, M. A., Hildemann, L. M., Cass, G. R., and Simoneit, B. R. T.:
939 Quantification of urban organic aerosols at a molecular level: Identification,
940 abundance and seasonal variation, Atmos. Environ., Part A, 27(8), 1309–1330,
941 1993a.
942 Rogge, W. F., Hildemann, L. M., Mazurek, M. A., Cass, G. R., and Simoneit, B. R. T.:
943 Sources of Fine Organic Aerosol. 2. Noncatalyst and Catalyst-Equipped Automobiles
944 and Heavy-Duty Diesel Trucks, Environ. Sci. Technol., 27(4), 636–651,
945 doi:10.1021/es00041a007, 1993b.
946 Saarikoski, S., Timonen, H., Saarnio, K.,Aurela, M., Jrvi, L., Keronen, P., Kerminen, V.
947 M., and Hillamo,R.:Sources of organic carbon in fine particulate matter in northern
948 European urban air, Atmos. Chem. Phys., 8, 6281-6295, 2008.
949 Salma, I., Németh, Z., Weidinger, T., Maenhaut, W.,Claeys, M.,Molnár,M.,Major,
950 I.,Ajtai, T.,Utry, N., and Bozóki,Z. : Source apportionment of carbonaceous
951 chemical species to fossil fuel combustion, biomass burning and biogenic emissions

by a coupled radiocarbon–levoglucosan marker method, Atmos. Chem. Phys., (17), 13767–13781, 2017.

Sandradewi, J., Prevot,A.S.H., Weingartner, E., Schmidhauser, R., Gysel, M., and Baltensperger,U.: A study of wood burning and traffic aerosols in an Alpine valley using a multi-wavelength Aethalometer, Atmos. Environ., 42, 101-112, 2008.

Seinfeld, J. H., and Pandis, S. N.: Atmospheric Chemistry and Physics: From Air Pollution to Climate Change, John Wiley & Sons, New York, 2nd edition, 1232 pp., ISBN-13: 978-0-471-72018-8, 2006.

Shen, G. F., Yuan, S. Y., Xie, Y., Xia, S. J., Li L., Yao, Y. K., Qiao, Y. Z., Zhang, J., Zhao, Q. Y., Ding, A. J., Li, B., and Wu, H. S: Ambient levels and temporal variations of PM2.5 and PM10 at a residential site in the mega-city, Nanjing, in the western Yangtze River Delta, China, J. Environ. Sci. Health, Part A 49, 171–178, 2014.

Sidhu, S., Gullett, B., Striebich, R., Klosterman, J., Contreras, J., and DeVito, M.: Endocrine disrupting chemical emissions from combustion sources: diesel particulate emissions and domestic waste open burn emissions, Atmos. Environ., 39(5), 801–811, 2005.

Simoneit, B. R. T.: The organic chemistry of marine sediments. In Chemical Oceanography, Riley J. P., Chester, R., Eds.; Academic Press:, New York., 1978.

Simoneit, B. R. T., Cardoso, J. N., and Robinson, N.: An assessment of terrestrial higher molecular weight lipid compounds in aerosol particulate matter over the south Atlantic from about 30-70° S, Chemosphere, 23(4), 447–465, 1991a.

Simoneit, B. R. T., Sheng, G. Y., Chen, X. J., Fu, J. M., Zhang, J., and Xu, Y. P.: Molecular marker study of extractable organic-matter in aerosols from urban areas of China, Atmos. Environ., Part A, 25(10), 2111–2129, 1991b.

Simoneit, B. R. T., Schauer, J. J., Nolte, C. G., Oros, D. R., Elias, V. O., Fraser, M. P., Rogge, W. F., and Cass, G. R.: Levoglucosan, a tracer for cellulose in biomass burning and atmospheric particles, Atmos. Environ., 33(2), 173–182, doi:10.1016/S1352-2310(98)00145-9, 1999.

Simoneit, B. R. T.: Biomass burning-a review of organic tracers for smoke from incomplete combustion, Appl. Geochem., 17, 129–162, 2002.

Simoneit, B. R. T., Elias, V. O., Kobayashi, M., Kawamura, K., Rushdi, A. I., Medeiros, P. M., Rogge, W. F., and Didyk, B. M.: Sugars-dominant water-soluble organic compounds in soils and characterization as tracers in atmospheric particulate matter, Environ. Sci. Technol., 38(22), 5939–5949, 2004a.

Simoneit, B. R. T., Kobayashi, M., Mochida, M., Kawamura, K., and Huebert, B. J.: Aerosol particles collected on aircraft flights over the northwestern Pacific region during the ACE-Asia campaign: Composition and major sources of the organic compounds, J. Geophys. Res.- Atmos., 109, D19S0, doi:10.1029/2004JD004565, 2004b.

Simoneit, B. R. T., Kobayashi, M., Mochida, M., Kawamura, K., Lee, M., Lim, H. J., Turpin, B. J., and Komazaki, Y.: Composition and major sources of organic compounds of aerosol particulate matter sampled during the ACE-Asia campaign, J. Geophys. Res.- Atmos., 109, D19S1, doi:10.1029/2004JD004598, 2004c.

Song, X. H., Polissar, A. V., and Hopke,P. K.: Sources of fine particle composition in the northeastern US, Atmos. Environ.,35(31), 5277–5286, 2001.

Stohl, A., Berg, T., Burkhart, J. F., Fjæraa, A. M., Forster, C., Herber, A., Hov Lunder, C., McMillan, W. W., Oltmans, S., Shiobara, M., Simpson, D., Solberg, S., Stebel, K., Str¨om, J., Tørseth, K., Treffeisen, R., Virkkunen, K., and Yttri, K. E.: Arctic

smoke - record high air pollution levels in the European Arctic due to agricultural fires in Eastern Europe in spring 2006, Atmos. Chem. Phys., 7, 511–534, 2007.

Teil, M.J., Blanchard, M., and Chevreuil,M.: Atmospheric fate of phthalate esters in an urban area (Paris—France),Sci. Total Environ., 354, 212–223, 2006.

Thuren, A., and Larsson,P.: Phthalate esters in the Swedish atmosphere,Environ. Sci. Technol., 24, 554–559, 1990.

Twomey, S.: The Influence of Pollution on the Shortwave Albedo of Clouds, J. Atmos. Sci., 34(7), 1149–1152, 1977.

Wang, G., Niu, S., Liu, C., and Wang, L.: Identification of dicarboxylic acids and aldehydes of PM_{10} and $PM_{2.5}$ aerosols in Nanjing, China, Atmos. Environ., 36(12), 1941–1950, doi:10.1016/S1352-2310(02)00180-2, 2002a.

Wang, G., Huang, L., Gao, S., Gao, S., and Wang, L.: Measurements of PM_{10} and $PM_{2.5}$ in urban area of Nanjing, China and the assessment of pulmonary deposition of particle mass, Chemosphere, 48(7), 689–695, doi:10.1016/S0045-6535(02)00197-2, 2002b.

Wang, G., and Kawamura, K.: Molecular characteristics of urban organic aerosols from Nanjing: A case study of a mega-city in China, Environ. Sci. Technol., 39(19), 7430–7438, 2005.

Wang, G., Kawamura, K., Lee, S., Ho, K. F., and Cao, J. J.: Molecular, seasonal, and spatial distributions of organic aerosols from fourteen Chinese cities, Environ. Sci. Technol., 40(15), 4619–4625, 2006.

Wang, G. H., Kawamura, K., Zhao, X., Li, Q. G., Dai, Z. X., and Niu, H. Y.: Identification, abundance and seasonal variation of anthropogenic organic aerosols from a mega-city in China, Atmos. Environ., 41(2), 407–416, doi:Doi 10.1016/J.Atmosenv.2006.07.033, 2007a.

Wang, G., Kawamura, K., Hatakeyama, S., Takami, A., Li, H., and Wang, W.: Aircraft measurement of organic aerosols over China, Environ. Sci. Technol., 41(9), 3115–3120, doi:10.1021/es062601h, 2007b.

Wang, G., Kawamura, K., Xie, M., Hu, S., Gao, S., Cao, J., An, Z., and Wang, Z.: Size-distributions of *n*-alkanes, PAHs and hopanes and their sources in the urban, mountain and marine atmospheres over East Asia, Atmos. Chem. Phys., 9(22), 8869–8882, 2009.

Wang, S., Xing, J., Jang, C., Zhu, Y., Full, J. S., and Hao, J.: Impact Assessment of Ammonia Emissions on Inorganic Aerosols in East China Using Response Surface Modeling Technique, Environ. Sci. Technol., 45 (21), 9293–9300, 2011.

Weschler, C. J.: Indoor–outdoor relationships for non-polar organic constituents of aerosol particles, Environ. Sci. Technol., 18, 648–652, 1984.

Xiao, Q., Ma, Z., Li, S., and Liu, Y.: The Impact of Winter Heating on Air Pollution in China, PLoS ONE 10(1): e0117311. doi:10.1371/journal. pone.0117311, 2015.

Yang, H., Yu, J. Z., Ho, S. S. H., Xu, J. H., Wu, W. S., Wan, C. H., Wang, X. D., Wang, X. R., and Wang, L. S.: The chemical composition of inorganic and carbonaceous materials in $PM_{2.5}$ in Nanjing, China, Atmos. Environ., 39(20), 3735–3749, 2005.

Yao, X., Lau, A. P. S., Fang, M., Chan, C. K., and Hu, M.: Size distributions and formation of ionic species in atmospheric particulate pollutants in Beijing, China: 2 - Dicarboxylic acids, Atmos. Environ., 37(21), 3001–3007, doi:10.1016/S1352-2310(03)00256-5, 2003.

Yttri, K. E., Dye, C., and Kiss, G.: Ambient aerosol concentrations of sugars and sugar-alcohols at four different sites in Norway, Atmos. Chem. Phys., 7, 4267–4279, 2007.

Zhang, R. Y., Suh, I., Zhao, J., Zhang, D., Fortner, E. C., Tie, X. X., Molina, L. T., and

Molina, M. J.: Atmospheric new particle formation enhanced by organic acids, Science (80-.)., 304(5676), 1487–1490, 2004.

Zhang, Q. J., Beekmann, M., Freney, E., Sellegri, K., Pichon, J. M., Schwarzenboeck, A., Colomb, A., Bourrianne, T., Michoud, V., and Borbon, A.: Formation of secondary organic aerosol in the Paris pollution plume and its impact on surrounding regions, Atmos. Chem. Phys., 15(24), 13973–13992, doi:10.5194/acp-15-13973-2015, 2015.

Zhang, Y., and Cao, F.: Fine particulate matter ($PM_{2.5}$) in China at a city level, Sci. Rep., 2015 DOI: 10.1038/srep14884.

Zhang, Y.-L., and Kawamura, K.: New directions: Need for better understanding of source and formation process of phthalic acid in aerosols as inferred from aircraft observations over China, Atmos. Environ., 140, 147–149, 2016.

Zheng, B., Zhang, Q., Zhang, Y., He, K. B., Wang, K., Zheng, G. J., Duan, F. K., Ma, Y. L., and Kimoto, T.: Heterogeneous chemistry: a mechanism missing in current models to explain secondary inorganic aerosol formation during the January 2013 haze episode in North China, Atmos. Chem. Phys., 15, 2031–2049, doi:10.5194/acp-15-2031-2015, 2015.

1113 **Table 1.** Mean concentrations of identified organic compound classes (ng m^{-3}) and
1114 carbonaceous components (μg m^{-3}) in the atmospheric aerosol samples (PM$_{2.5}$) from Nanjing,
1115 China.
1116

Compounds	Daytime				Nighttime			
	Mean	Min[a]	Max[b]	SD[c]	Mean	Min[a]	Max[b]	SD[c]
n-Alkanes	177	96.1	467	76.6	218	74.4	500	89.3
Plant Wax Alkanes	15.5	1.12	56.2	11.2	17.6	0	62.1	14.2
Fatty acids	66.8	14.3	254	47.9	91.3	8.57	252	59.2
Fatty alcohols	36.9	7.30	165	29.9	43.8	4.61	129	26.7
Anhydro-sugars	42.3	5.8	191	40.9	71.2	5.71	367	80.1
Sugars	3.44	0.78	8.89	1.75	3.43	0.59	8.49	1.81
Phthalate esters	13.9	2.66	40.0	10.1	16.3	3.80	51.8	11.1
Glycerol and polyacids	7.78	1.59	29.7	6.17	9.30	2.54	23.1	5.79
Aromatic acids	6.70	1.53	23.1	4.69	8.37	1.99	18.4	4.83
Lignin and resin products	2.68	0.84	6.96	1.29	3.39	0.75	14.3	2.70
PAHs	54.5	29.5	106	17.8	74.8	21.7	223	43.8
Hopanes	3.79	0.07	20.8	4.15	4.64	0.13	26.1	5.31
Steranes	2.29	1.13	9.15	1.56	2.65	1.08	11.1	1.92
Total organics	**434**	**163**	**1378**	**254**	**565**	**126**	**1686**	**347**
OC	18.6	8.76	40.0	8.44	19.1	2.98	40.1	8.53
EC	8.25	2.41	30.3	5.46	8.86	8.86	8.86	8.86
WSOC	11.7	5.52	26.6	4.68	18.1	1.51	34.4	8.92
OC/EC	2.47	1.30	3.69	0.54	2.36	1.51	3.76	0.56
WSOC/OC	0.58	0.42	0.78	0.10	0.55	0.40	0.70	0.08

1117 [a]Minimum, [b]Maximum, [c]Standard deviation

1143 **Table 2.** Comparisons of the average concentrations (ng m^{-3}) of organic tracers with those
1144 measured during 2004-2005 (Wang and Kawamura, 2005; Wang et al., 2007a[b]) in Nanjing
1145 aerosols during winter.
1146

Compounds	This study		2004-2005	
	Daytime	Nighttime	Daytime	Nighttime
n-Alkanes	177	218	172	278
Plant Wax Alkanes	15.5	17.6	18.8	20.6
Fatty acids	66.8	91.3	245	338
Fatty alcohols	36.9	43.8	74.5	120
Levoglucosan	42.3	71.2	238	297
Sugars	3.44	3.43	59	53
Phthalate esters[b]	13.9	16.3	158	181
Glycerol and polyacids	7.78	9.30	41.4	41.8
Aromatic acids	6.70	8.37		Not detected
Lignin and resin products	2.68	3.39	16.0	35.1
PAHs[b]	54.5	74.8	69	104
Hopanes[b]	3.79	4.64	7.3	9.9
Steranes	2.29	2.65		Not detected
Total organics	**434**	**565**	**1108**	**1502**

1154 **Table 3.** Diagnostic concentration ratios of biomarkers for source identification from fossil fuel
1155 combustions including gasoline- and diesel cars.
1156

	Present study		Gasoline		Diesel	Coal
	Daytime	Nighttime	Noncatalyst	Catalyst		
IP/BghiP	1.26	1.19	0.22[a]		0.50[a]	1.3[a]
BghiP/Bep	1.21	1.13	2.0[b]			0.8[b]
Flut/(Flut + IP)	0.57	0.56	0.46-0.56[c]	0.44[c]		
IP/(IP + BghiP)	0.56	0.54	0.18[c]		0.37[c]	0.56[c]
$C_{29}\alpha\beta/C_{30}\alpha\beta$	0.65	0.51	0.59[d]	0.66[d]	0.42[d]	0.58-2.0[e]
$C_{31}\alpha\beta S/(C_{31}\alpha\beta S + C_{31}\alpha\beta R)$	0.39	0.57	0.60[d]	0.62[d]	0.50[d]	0.05-0.37[e]

[a]Grimmer et al., 1983, [b]Ohura et al., 2004, [c]Bi et al., 2005, [d]Rogge et al., 1993a, [e]Oros and Simoneit, 2000

1159

1160

1161

1162

1163 **Figure 1.** A map of sampling site located in Nanjing, China.
1164
1165
1166
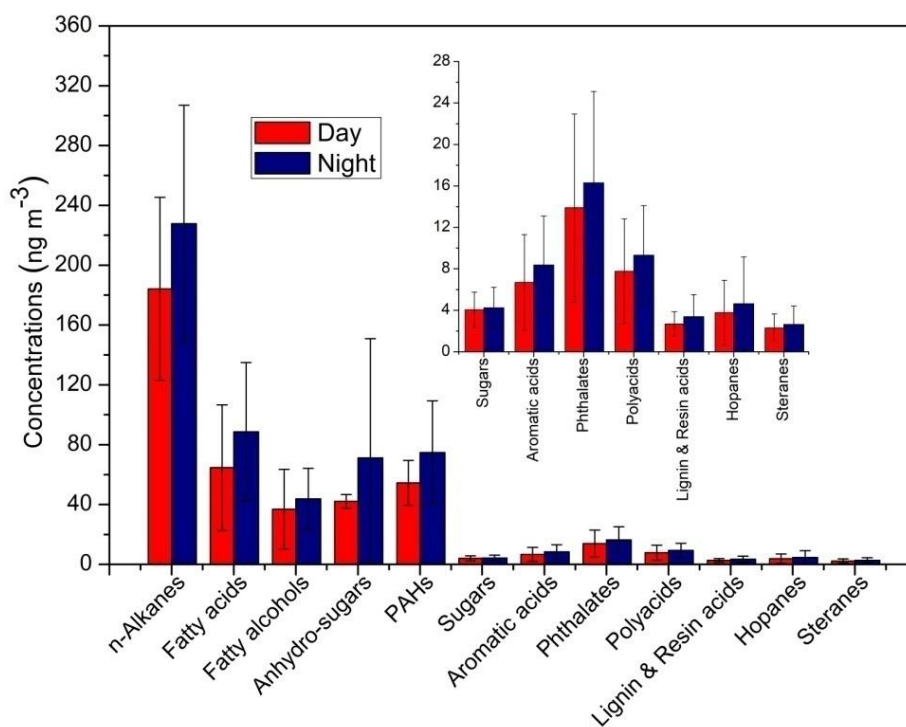
1167

1168 **Figure 2.** Concentrations of organic compound classes detected in the Nanjing
1169 aerosols.
1170

1171

1172

1173

1174
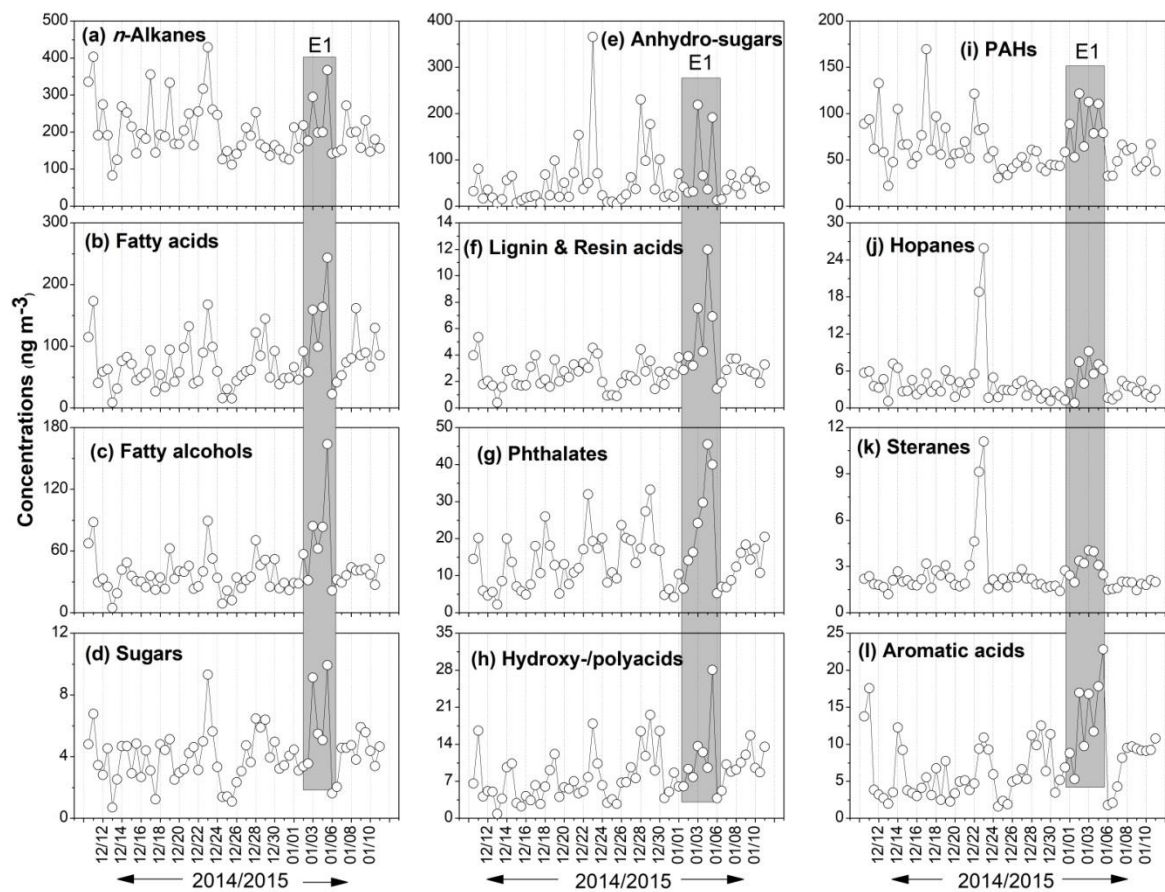
1175

Figure 3. Temporal variations in the concentrations of organic compound classes detected in the Nanjing urban aerosols.

1176
1177
1178

1179
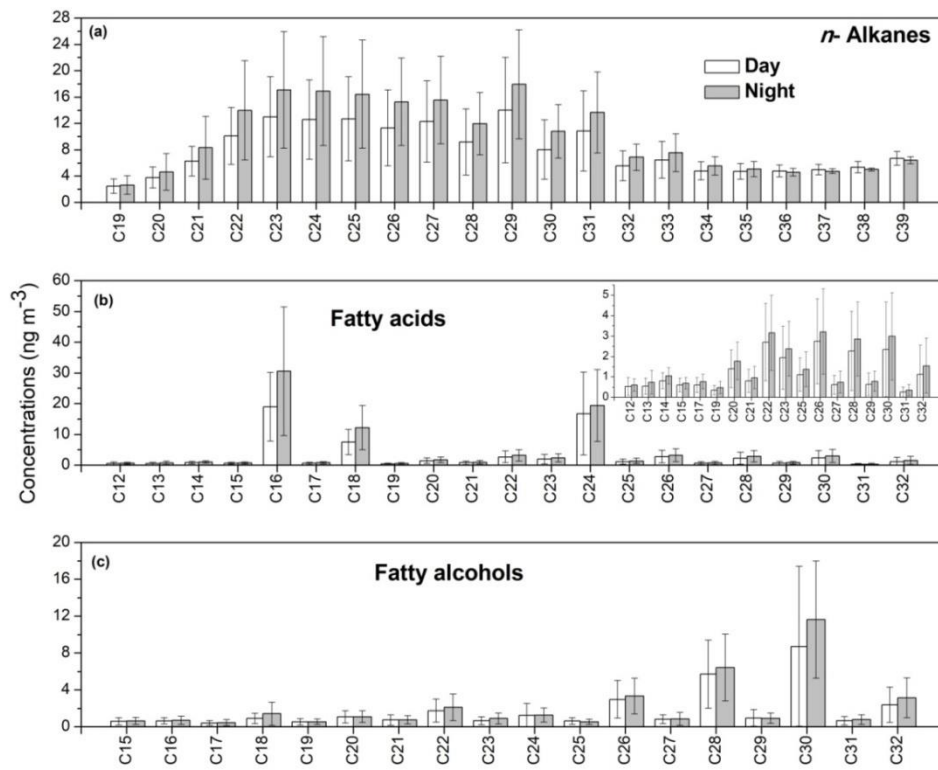
1180

1181 **Figure 4.** Molecular distributions of *n*-alkanes, fatty acids and fatty alcohols in PM$_{2.5}$
1182 aerosols collected from Nanjing, China. Inner panel of b represent correspondence
1183 carbon of fatty alcohols which concentrations are low.

1184

1185
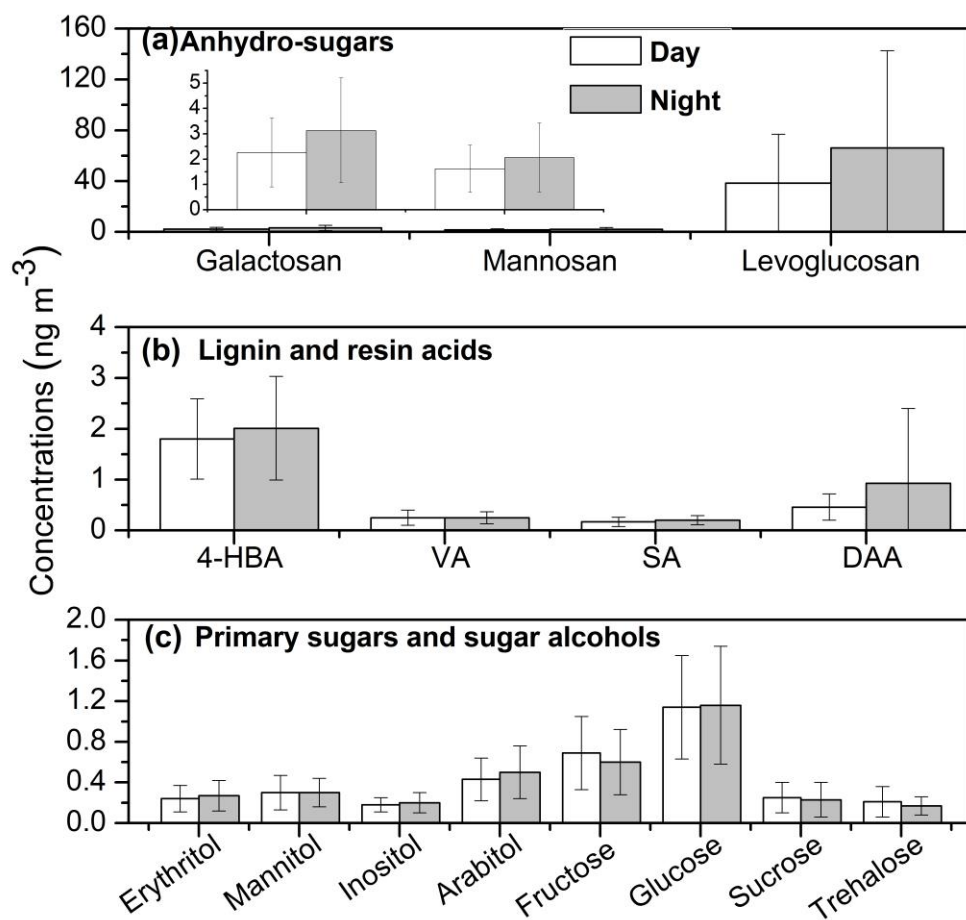
1186

Figure 5. Molecular distributions of anhydro-sugars, lignin and resin acids and sugars/sugar alcohols in Nanjing aerosols. [4-HBA: 4-hydroxybenzoic acid , VA: vanillic acid, SA: syringic acid and DAA: dehydroabietic acid].
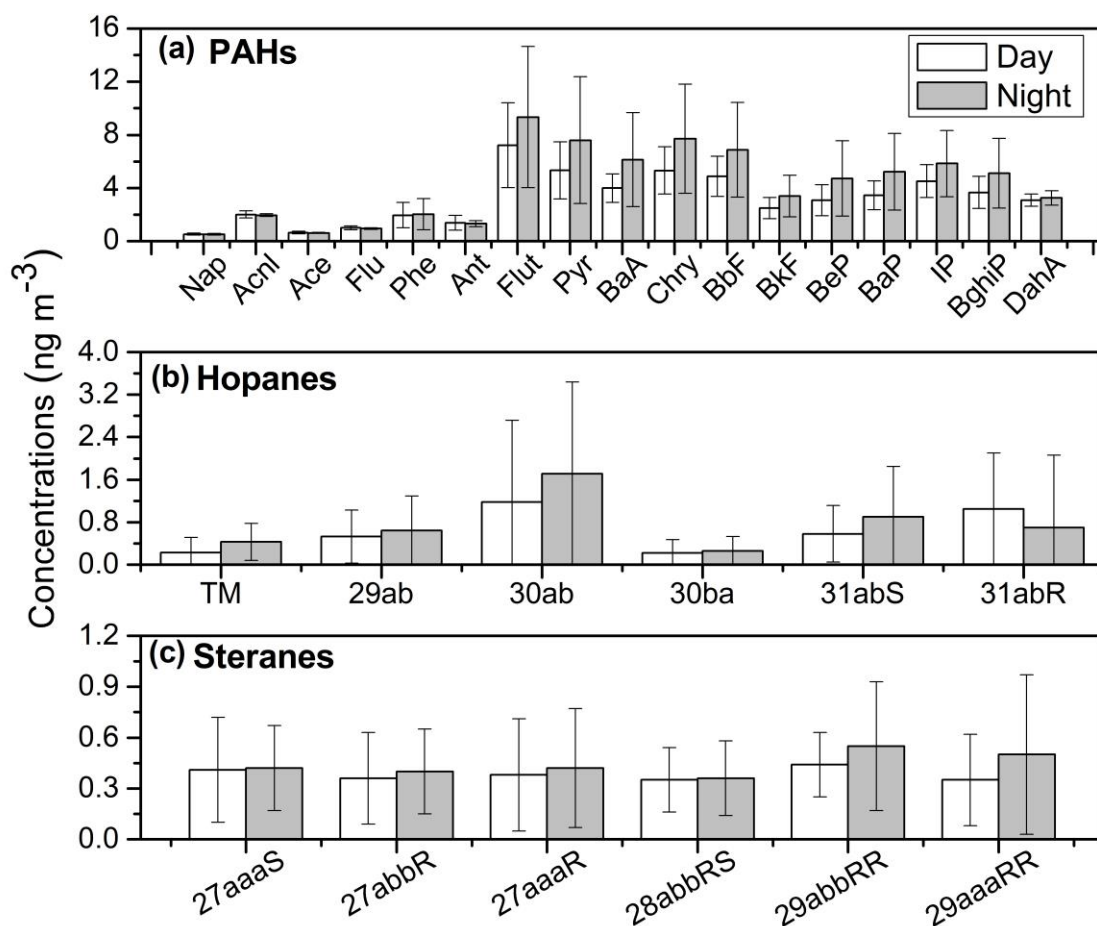
1191

Figure 6. Molecular distributions of PAHs, hopanes and steranes in winter aerosols from Nanjing, China. [Abbreviation of PAHs: napthalene, Nap; acenaphthylene, Acnl; acenapthene, Ace; fluorene, Flu; phenanthrene, Phe; anthracene, Ant; fluoranthene, Flut; pyrene, Pyr; benzo[a]anthracene, BaA; chrysene, Chry; benzo(b)fluoranthene, BbF; benzo(k)fluoranthene, BkF ; benzo(e)pyrene, BeP; benzo(a)pyrene, BaP; indeno(1,2,3-cd)pyrene, IP; benzo(ghi)perylene, BghiP; Dibenzo[a,h] anthracene, DahA].
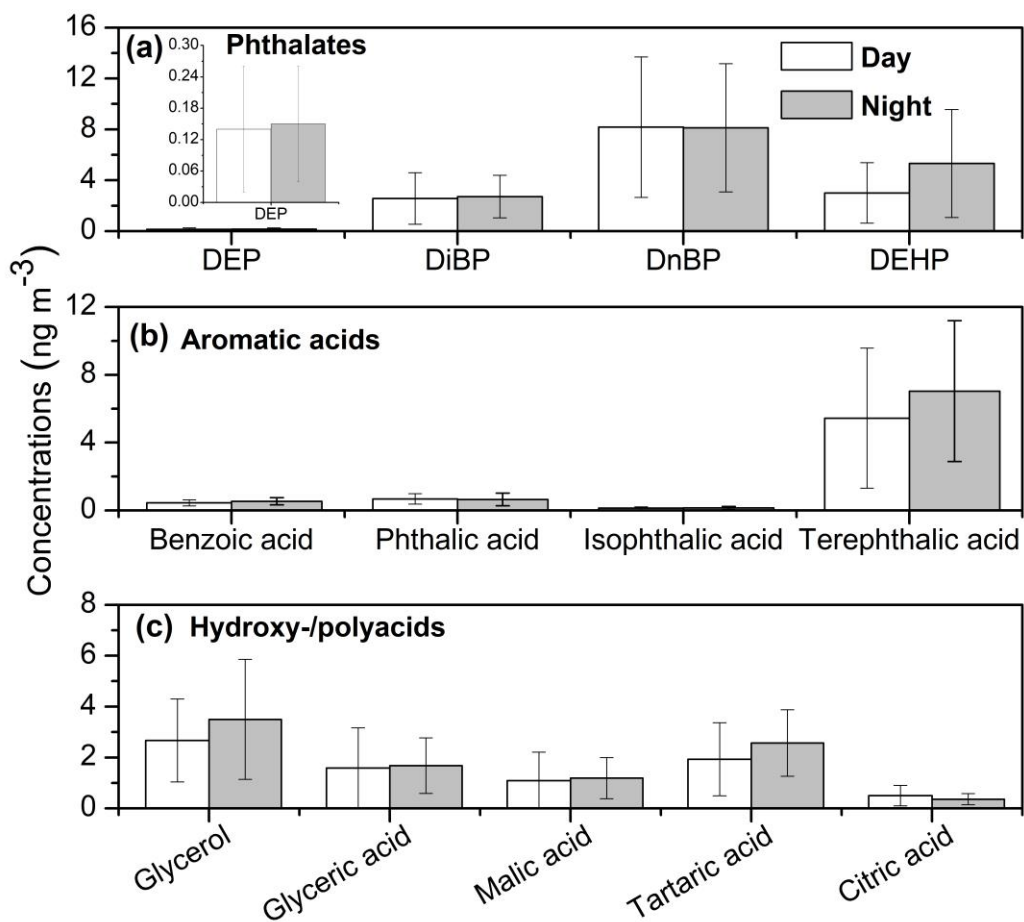
1199

1200 **Figure 7.** Molecular distributions of phthalates, aromatic acids and hydroxy-/polyacids in
1201 Nanjing aerosols.
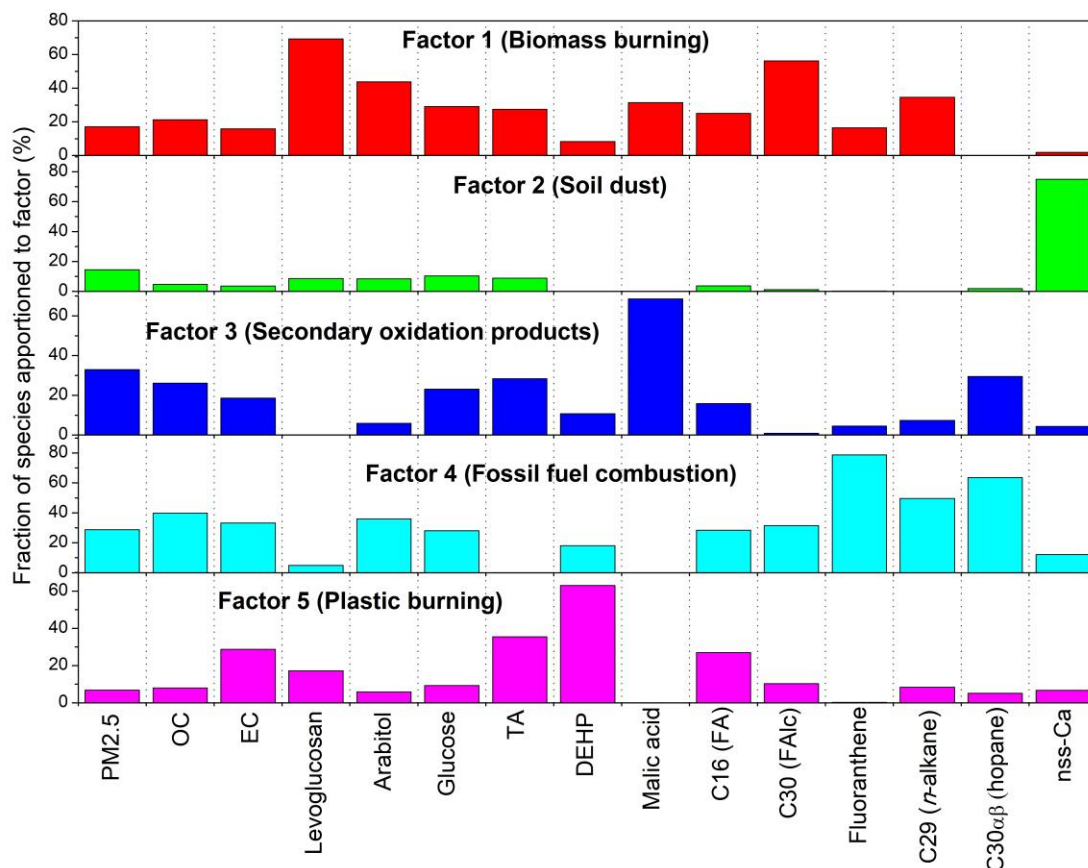
1202
1203 **Figure 8.** Composition profiles (% of total of each species) for the five factors resolved
1204 by PMF based on data from Nanjing winter aerosols from 11 December 2014 to 11
1205 January 2015. [TA: terephthalic acid, DEHP: di-(2-ethylhexyl) phthalate, FA: fatty acid, FAlc: fatty
1206 alcohol].

1207

1208
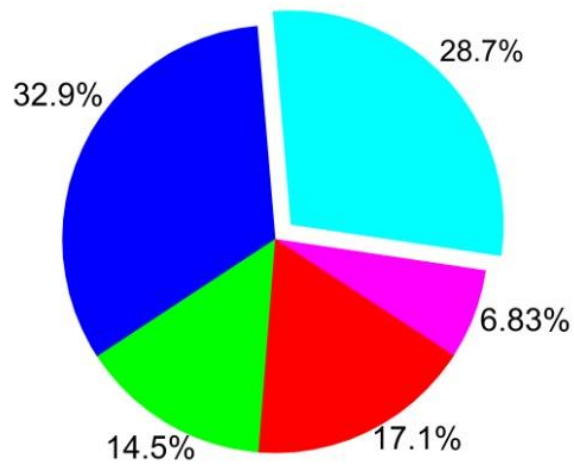
Figure 9. Pie diagrams showing the estimated source contributions of five factors resolved by PMF to the $PM_{2.5}$ in Nanjing aerosols.

1   Supporting information for

2   **Characterization of organic aerosols from a Chinese Mega-City during winter:**
3   **predominance of fossil fuel combustion**

5   **Md. Mozammel Haque[1,2,3], Kimitaka Kawamura[2], Dhananjay K. Deshmukh[2], Cao**
6   **Fang[1, 3], Wenhuai Song[1,3], Bao Mengying[1,3] and Yan-Lin Zhang[1,3*]**

8   *[1] Yale-NUIST Center on Atmospheric Environment, Department of Applied Meteorology,*
9   *Nanjing University of Information Science and Technology, Nanjing 10044, China*
10   *[2] Chubu Institute for Advanced Studies, Chubu University, Kasugai 487-8501, Japan*
11   *[3]Key Laboratory of Meteorological Disaster, Ministry of Education & Collaborative*
12   *Innovation Center on Forecast and Evaluation of Meteorological Disasters, Nanjing*
13   *University of Information Science and Technology, Nanjing 10044, China*

16   *Corresponding author: Yan-Lin Zhang

17   E-mail: dryanlinzhang@outlook.com

Table S1. Concentrations of identified organic compounds (ng m^{-3}) in the atmospheric aerosol samples (PM$_{2.5}$) from Nanjing, China.

Compounds	Daytime				Nighttime			
	Mean	Min[a]	Max[b]	SD[c]	Mean	Min[a]	Max[b]	SD[c]
n-Alkanes								
C_{13}	1.91	1.59	3.27	0.29	1.93	1.58	3.50	0.39
C_{14}	1.24	0.89	2.16	0.27	1.17	0.93	1.79	0.22
C_{15}	1.26	0.82	1.97	0.25	1.11	0.77	1.60	0.23
C_{16}	0.35	0.00	0.88	0.27	0.32	0.00	0.96	0.28
C_{17}	1.04	0.37	2.41	0.45	0.99	0.39	1.99	0.34
C_{18}	1.11	0.32	2.66	0.48	1.22	0.58	2.78	0.48
C_{19}	2.50	1.17	5.69	1.11	2.65	1.05	7.30	1.42
C_{20}	3.79	1.09	7.99	1.60	4.64	1.01	15.5	2.76
C_{21}	6.28	3.30	12.9	2.26	8.31	2.50	25.7	4.75
C_{22}	10.1	5.02	27.5	4.31	14.0	2.77	33.7	7.53
C_{23}	13.0	6.10	38.5	6.08	17.1	3.22	44.6	8.86
C_{24}	12.6	6.59	36.0	6.03	16.9	2.94	46.1	8.27
C_{25}	12.7	5.57	36.4	6.39	16.4	2.60	44.6	8.21
C_{26}	11.3	4.97	28.9	5.77	15.3	3.43	34.9	6.62
C_{27}	12.3	5.25	33.7	6.19	15.6	2.97	32.9	6.65
C_{28}	9.19	4.80	29.3	5.01	11.9	3.14	24.2	4.74
C_{29}	14.0	5.76	44.9	8.00	17.9	3.05	43.5	8.27
C_{30}	8.03	4.36	25.9	4.51	10.8	3.20	21.8	4.06
C_{31}	10.9	4.80	35.9	6.06	13.7	4.01	35.6	6.15
C_{32}	5.56	3.09	14.9	2.28	6.87	4.18	13.1	1.98
C_{33}	6.48	4.01	18.5	2.79	7.55	3.55	18.5	2.87
C_{34}	4.80	3.57	9.94	1.36	5.56	4.04	10.2	1.40
C_{35}	4.73	3.61	9.29	1.20	5.06	3.80	9.37	1.15
C_{36}	4.77	4.10	8.02	0.91	4.61	3.95	6.78	0.57
C_{37}	5.00	4.35	8.80	0.80	4.76	4.35	5.97	0.35
C_{38}	5.35	4.67	9.46	0.85	5.01	4.75	5.53	0.20
C_{39}	6.71	5.89	11.6	1.04	6.41	5.64	7.79	0.53
Subtotal	177	96.1	467	76.6	218	74.4	500	89.3
CPI (C_{20}–C_{39})	1.28	1.18	1.32	1.32	1.24	1.10	1.37	1.35
Plant Wax Alkanes								
C_{23}	1.64	0.30	6.72	1.19	1.80	0.00	4.98	1.56
C_{25}	0.81	0.00	3.93	0.82	0.76	0.00	4.13	1.07
C_{27}	2.02	0.00	5.28	1.18	2.00	0.00	5.69	1.65
C_{29}	5.42	0.47	17.4	3.58	6.55	0.00	20.5	4.47
C_{31}	4.08	0.25	15.5	2.87	4.82	0.00	18.2	3.54
C_{33}	1.30	0.10	6.05	1.15	1.36	0.00	6.85	1.38
C_{35}	0.16	0.00	0.86	0.26	0.22	0.00	1.04	0.33
C_{37}	0.10	0.00	0.53	0.17	0.10	0.00	0.74	0.19
Subtotal	15.5	1.12	56.2	11.2	17.6	0	62.1	14.2

    Table 1. (Continued)

Compounds	Daytime				Nighttime			
	Mean	Min[a]	Max[b]	SD[c]	Mean	Min[a]	Max[b]	SD[c]
		Fatty acids						
$C_{12:0}$	0.54	0.12	2.04	0.44	0.60	0.19	1.57	0.31
$C_{13:0}$	0.55	0.11	2.08	0.40	0.74	0.03	2.38	0.57
$C_{14:0}$	0.81	0.27	2.48	0.39	1.05	0.21	1.87	0.40
$C_{15:0}$	0.61	0.19	1.88	0.34	0.69	0.05	1.50	0.29
$C_{16:0}$	18.9	5.12	56.8	11.2	30.5	3.87	89.2	20.9
$C_{17:0}$	0.60	0.18	1.99	0.37	0.77	0.11	1.80	0.36
$C_{18:0}$	7.46	1.88	23.4	4.11	12.2	1.48	28.9	7.16
$C_{19:0}$	0.36	0.08	1.07	0.23	0.48	0.02	1.41	0.30
$C_{20:0}$	1.40	0.38	5.06	0.92	1.78	0.18	4.19	0.92
$C_{21:0}$	0.81	0.14	2.87	0.57	0.96	0.03	2.32	0.55
$C_{22:0}$	2.70	0.57	10.4	1.90	3.16	0.17	7.51	1.85
$C_{23:0}$	1.94	0.43	8.47	1.55	2.38	0.10	5.41	1.34
$C_{24:0}$	16.8	3.28	73.8	13.5	19.4	1.51	50.9	11.7
$C_{25:0}$	1.11	0.16	4.34	0.82	1.37	0.00	3.45	0.85
$C_{26:0}$	2.75	0.37	10.6	2.08	3.22	0.10	9.07	2.09
$C_{27:0}$	0.62	0.09	1.94	0.46	0.74	0.00	2.07	0.54
$C_{28:0}$	2.27	0.38	10.3	1.95	2.86	0.23	6.88	1.81
$C_{29:0}$	0.63	0.09	2.88	0.56	0.79	0.00	2.10	0.49
$C_{30:0}$	2.35	0.34	12.6	2.32	2.99	0.17	9.40	2.14
$C_{31:0}$	0.26	0.00	1.38	0.25	0.35	0.05	1.17	0.28
$C_{32:0}$	1.13	0.00	7.48	1.44	1.55	0.07	6.04	1.35
$C_{18:1}$	0.36	0.04	1.62	0.33	0.39	0.00	1.66	0.37
$C_{18:2}$	1.81	0.10	8.18	1.80	2.31	0.00	10.9	2.58
Subtotal	66.8	14.3	254	47.9	91.3	8.57	252	59.2
CPI ($C_{20:0}$-$C_{32:0}$)	5.41	4.24	6.50	0.54	5.52	4.29	13.2	1.51
		Fatty alcohols						
C_{12}	1.74	0.26	5.76	1.12	1.99	0.16	7.33	1.38
C_{14}	3.58	0.70	23.9	4.11	4.13	0.10	11.6	2.60
C_{15}	0.60	0.22	1.81	0.39	0.66	0.05	1.33	0.38
C_{16}	0.66	0.16	1.60	0.34	0.71	0.05	2.32	0.45
C_{17}	0.42	0.10	1.30	0.26	0.46	0.13	1.98	0.34
C_{18}	0.91	0.19	2.33	0.57	1.43	0.13	6.35	1.25
C_{19}	0.54	0.15	2.09	0.35	0.56	0.15	1.34	0.30
C_{20}	1.08	0.18	2.71	0.66	1.11	0.27	3.06	0.63
C_{21}	0.74	0.15	2.98	0.56	0.75	0.12	2.12	0.45
C_{22}	1.76	0.47	6.37	1.26	2.11	0.13	6.92	1.44
C_{23}	0.68	0.14	1.97	0.43	0.92	0.23	2.92	0.60
C_{24}	1.22	0.19	7.86	1.31	1.28	0.16	3.50	0.77
C_{25}	0.64	0.21	1.94	0.35	0.55	0.11	1.26	0.27
C_{26}	2.99	0.18	10.7	2.03	3.34	0.68	7.77	1.93
C_{27}	0.83	0.19	2.27	0.48	0.87	0.00	3.74	0.70
C_{28}	5.72	1.17	19.3	3.69	6.44	1.09	18.7	3.62

Compounds	Daytime				Nighttime			
	Mean	Min[a]	Max[b]	SD[c]	Mean	Min[a]	Max[b]	SD[c]
C_{29}	0.97	0.16	5.20	0.90	0.94	0.00	2.38	0.55
C_{30}	8.73	1.87	51.7	8.66	11.6	0.87	32.6	6.36
C_{31}	0.67	0.00	2.46	0.47	0.78	0.00	2.86	0.51
C_{32}	2.39	0.61	10.4	1.91	3.14	0.18	9.29	2.15
Subtotal	36.9	7.30	165	29.9	43.8	4.61	129	26.7
CPI (C_{20}-C_{32})	5.22	2.56	10.3	1.67	6.32	3.06	15.5	2.45
Anhydro-sugars								
Galactosan	2.26	0.65	7.47	1.36	3.13	0.48	7.75	2.07
Mannosan	1.62	0.36	4.30	0.93	2.06	0.27	5.73	1.36
Levoglucosan	38.4	4.79	179	38.6	66.0	4.96	354	76.7
Subtotal	42.3	5.8	191	40.9	71.2	5.71	367	80.1
Sugars								
Erythritol	0.24	0.04	0.64	0.13	0.27	0.02	0.58	0.15
Mannitol	0.30	0.09	0.91	0.17	0.30	0.07	0.70	0.14
Inositol	0.18	0.05	0.40	0.07	0.20	0.05	0.43	0.10
Arabitol	0.43	0.08	1.20	0.21	0.50	0.04	1.10	0.26
Fructose	0.69	0.15	1.45	0.36	0.60	0.11	1.50	0.32
Glucose	1.14	0.27	2.77	0.51	1.16	0.20	2.86	0.58
Sucrose	0.25	0.05	0.71	0.15	0.23	0.06	0.87	0.17
Trehalose	0.21	0.05	0.81	0.15	0.17	0.04	0.45	0.09
Subtotal	3.44	0.78	8.89	1.75	3.43	0.59	8.49	1.81
Phthalate esters								
Diethyl (DEP)	0.14	0.03	0.57	0.12	0.15	0.03	0.50	0.11
Diisobutyl (DiBP)	2.56	0.59	8.54	2.03	2.72	0.63	7.19	1.67
Di-n-butyl (DnBP)	8.18	1.30	20.0	5.52	8.12	2.08	22.8	5.04
Di-(2-ethylhexyl) (DEHP)	3.00	0.74	10.9	2.38	5.32	1.06	21.3	4.24
Subtotal	13.9	2.66	40.0	10.1	16.3	3.80	51.8	11.1
Glycerol and Polyacids								
Glycerol	2.67	0.66	5.99	1.63	3.50	0.73	8.72	2.36
Glyceric acid	1.59	0.28	8.34	1.58	1.68	0.34	4.30	1.09
Malic acid	1.09	0.07	4.66	1.12	1.19	0.36	3.35	0.81
Tartaric acid	1.93	0.51	8.57	1.44	2.57	1.02	5.74	1.31
Citric acid	0.50	0.07	2.15	0.40	0.36	0.09	0.98	0.22
Subtotal	7.78	1.59	29.7	6.17	9.30	2.54	23.1	5.79
Aromatic acids								
Benzoic acid	0.45	0.17	0.95	0.18	0.54	0.24	1.22	0.21
Phthalic acid	0.68	0.24	1.24	0.30	0.65	0.28	1.80	0.37
Isophthalic acid	0.13	0.03	0.33	0.08	0.14	0.05	0.40	0.10
Terephthalic acid	5.44	1.09	20.6	4.13	7.04	1.42	15.0	4.15
Subtotal	6.70	1.53	23.1	4.69	8.37	1.99	18.4	4.83

 Table 1. (Continued)

Compounds	Daytime				Nighttime			
	Mean	Min[a]	Max[b]	SD[c]	Mean	Min[a]	Max[b]	SD[c]
				Lignin and Resin products				
4-Hydroxybenzoic acid	1.80	0.65	4.31	0.79	2.01	0.62	4.96	1.02
Vanillic acid	0.25	0.04	0.92	0.15	0.25	0.08	0.66	0.12
Syringic acid	0.17	0.04	0.57	0.09	0.20	0.05	0.43	0.09
Dehydroabietic acid	0.46	0.11	1.16	0.26	0.93	0.00	8.29	1.47
Subtotal	2.68	0.84	6.96	1.29	3.39	0.75	14.3	2.70
				PAHs				
Napthalene (Nap)	0.52	0.45	0.80	0.07	0.51	0.41	0.60	0.05
Acenaphthylene (Acnl)	2.01	1.80	3.47	0.28	1.95	1.66	2.17	0.10
Acenapthene (Ace)	0.64	0.56	1.22	0.11	0.61	0.55	0.69	0.04
Fluorene (Flu)	1.00	0.83	1.70	0.14	0.94	0.85	1.05	0.05
Phenanthrene (Phe)	1.95	0.68	4.52	0.96	2.03	0.33	4.62	1.17
Anthracene (Ant)	1.38	1.11	4.21	0.56	1.30	1.00	2.02	0.23
Fluoranthene (Flut)	7.21	3.01	18.2	3.19	9.34	2.14	27.6	5.33
Pyrene (Pyr)	5.33	2.15	11.4	2.15	7.59	1.32	26.8	4.78
Benzo[a]anthracene (BaA)	3.98	2.37	6.44	1.07	6.14	1.87	14.8	3.54
Chrysene (Chry)	5.31	2.50	9.11	1.78	7.70	1.24	17.0	4.11
Benzo[b]fluoranthene (BbF)	4.88	2.42	8.40	1.52	6.88	1.51	14.4	3.57
Benzo[k]fluoranthene (BkF)	2.47	0.94	4.28	0.80	3.39	0.84	7.19	1.56
Benzo[e]pyrene (BeP)	3.08	1.39	6.01	1.18	4.71	0.68	11.6	2.84
Benzo[a]pyrene (BaP)	3.46	1.86	6.35	1.08	5.23	1.31	13.1	2.88
Indeno[1,2,3-cd]pyrene (IP)	4.52	2.85	8.01	1.24	6.50	2.11	24.5	4.21
Benzo[ghi]perylene (BghiP)	3.66	1.91	6.93	1.22	5.85	1.40	26.1	4.64
Dibenzo[a,h]anthracene (DahA)	3.08	2.70	5.19	0.46	4.11	2.49	28.7	4.68
Subtotal	54.5	29.5	106	17.8	74.8	21.7	223	43.8
				Hopanes				
17 α(H)-22,29,30-Trisnorhopane	0.23	0.00	1.51	0.28	0.43	0.03	1.46	0.35
17 α(H)-21 β(H)-30-Norhopane	0.53	0.03	2.65	0.50	0.64	0.03	3.39	0.65
17 α(H)-21 β(H)-Hopane	1.18	0.02	8.91	1.54	1.71	0.07	8.88	1.73
17 β(H)-21 α(H)-Hopane	0.22	0.01	1.12	0.25	0.26	0.00	0.93	0.27
17 α(H)-21 β(H)-22S-Homohopane	0.58	0.00	2.07	0.53	0.90	0.00	3.94	0.95
17 α(H)-21 β(H)-22R-Homohopane	1.05	0.01	4.58	1.05	0.70	0.00	7.52	1.36
Subtotal	3.79	0.07	20.8	4.15	4.64	0.13	26.1	5.31
				Steranes				
ααα 20S-Cholestane	0.41	0.19	1.64	0.31	0.42	0.18	1.42	0.25
αββ 20R-Cholestane	0.36	0.18	1.74	0.27	0.40	0.17	1.43	0.25
ααα 20R-Cholestane	0.38	0.18	1.98	0.33	0.42	0.18	2.01	0.35
αββ 20R, 24S-Methylcholestane	0.35	0.19	1.13	0.19	0.36	0.16	1.25	0.22
αββ 20R, 24R-Ethylcholestane	0.44	0.22	1.06	0.19	0.55	0.23	2.34	0.38
ααα 20R, 24R-Ethylcholestane	0.35	0.17	1.60	0.27	0.50	0.16	2.65	0.47
Subtotal	2.29	1.13	9.15	1.56	2.65	1.08	11.1	1.92

[a]Minimum, [b]Maximum, [c]Standard deviation
CPI: carbon preference index: $(C_{21}+C_{23}+C_{25}+C_{27}+C_{29}+C_{31}+C_{33}+C_{35}+C_{37}+C_{39})/(C_{20}+C_{22}+C_{24}+C_{26}+C_{28}+C_{30}+C_{32}+C_{34}+C_{36}+C_{38})$ for n-alkanes;
$(C_{20}+C_{22}+C_{24}+C_{26}+C_{28}+C_{30}+C_{32})/(C_{21}+C_{23}+C_{25}+C_{27}+C_{29}+C_{31})$ for fatty acids; $(C_{20}+C_{22}+C_{24}+C_{26}+C_{28}+C_{30}+C_{32})/(C_{21}+C_23+C_{25}+C_{27}+C_{29}+C_{31})$ for fatty alcohols.
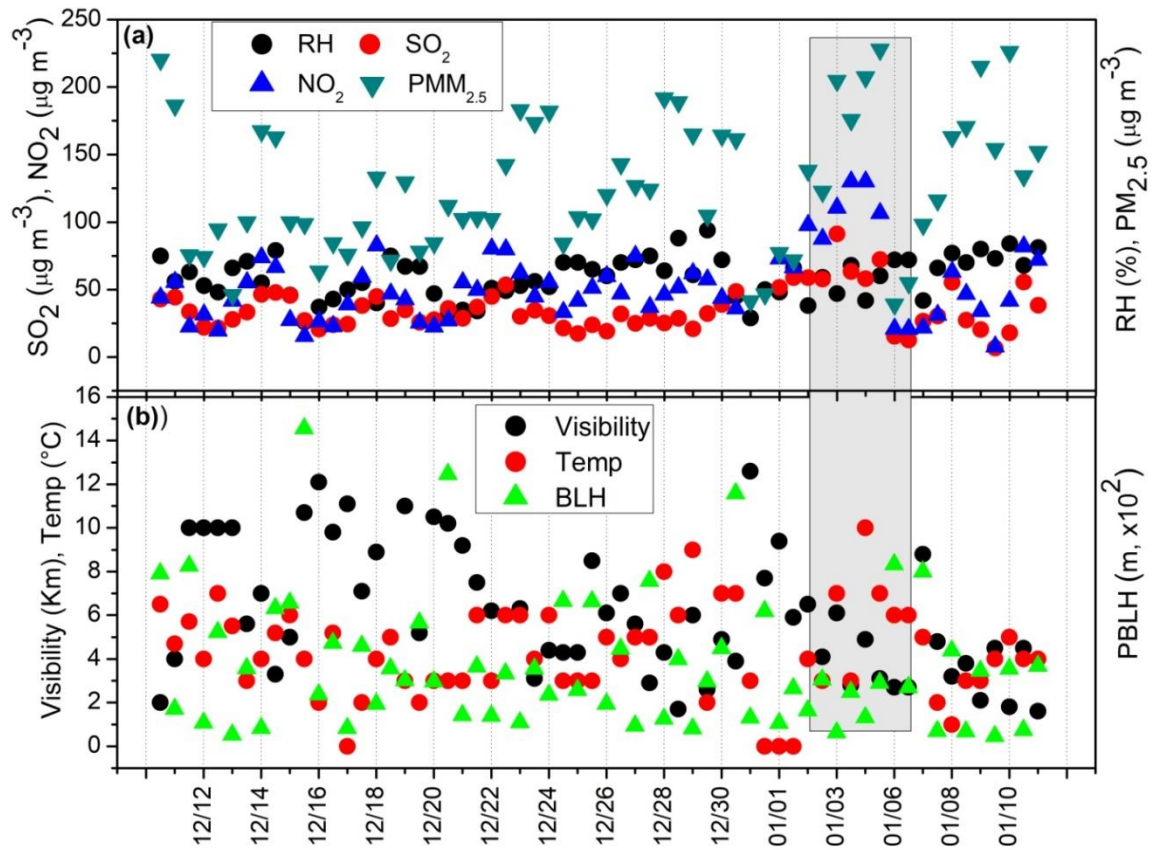
Figure S1. Diurnal variations of (a) SO$_2$, NO$_2$, Relative Humidity (RH), and PM$_{2.5}$ (b) Visibility, Temperature (Temp) and Planetary Boundary Layer Height (PBLH) in Nanjing aerosols during study period.

46
47
48
49
50
51
52
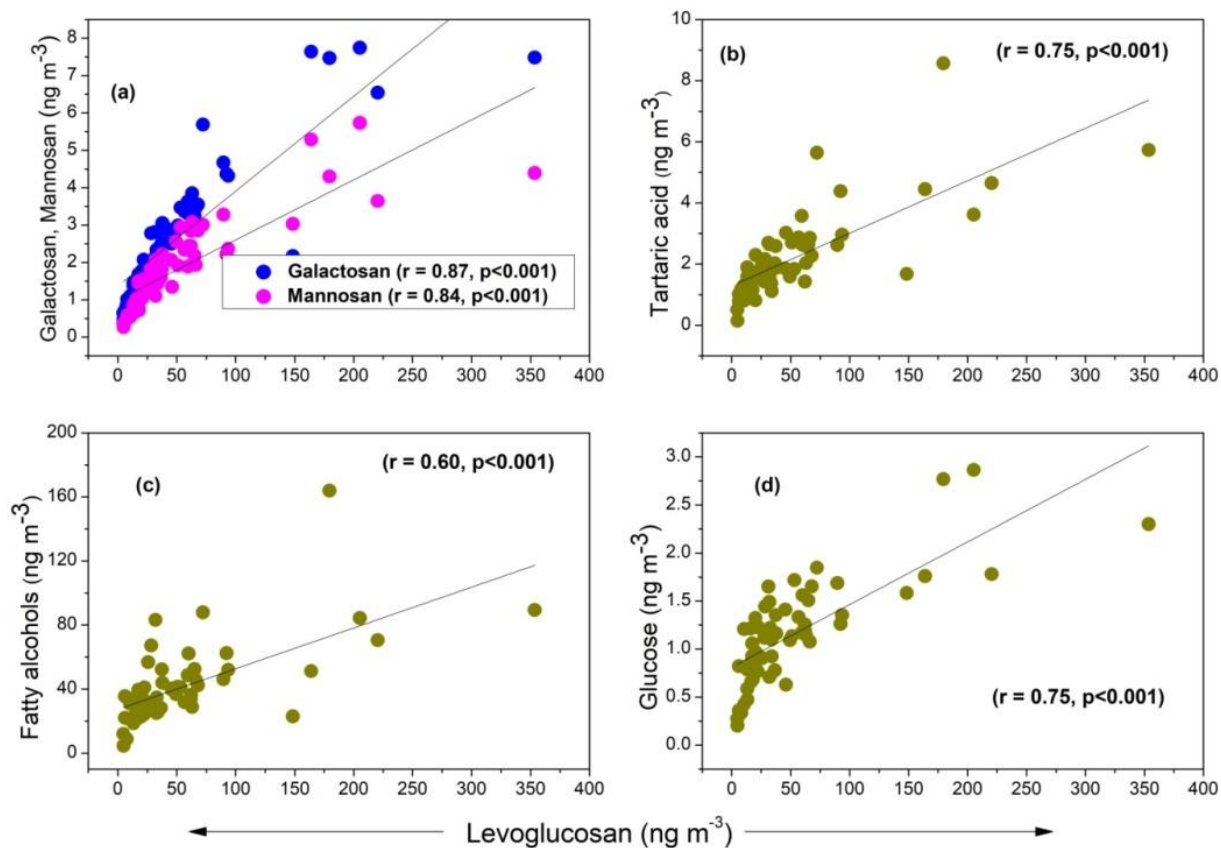
Figure S2. Correlation coefficients of levoglucosan with galactosan, mannosan, glucose, tartaric acid
and fatty alcohols in urban aerosols in Nanjing.
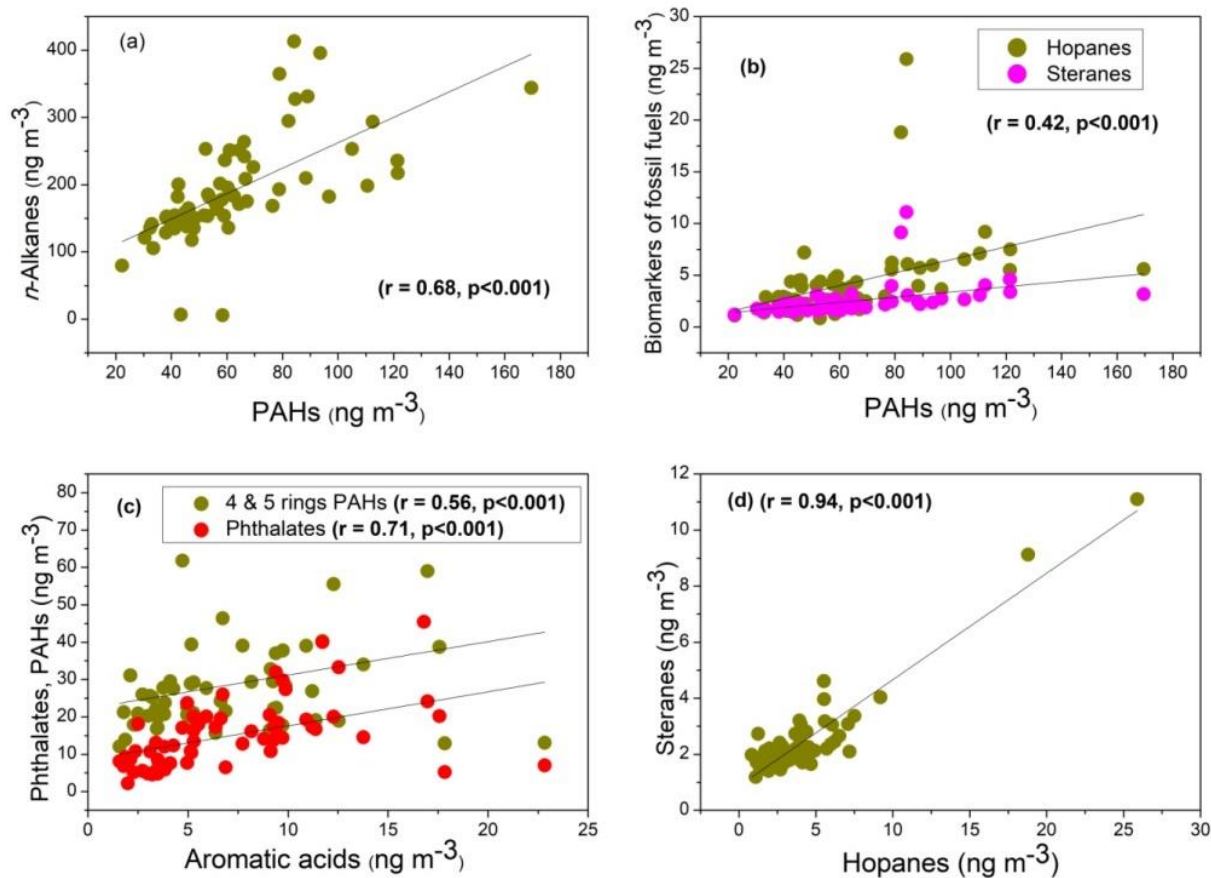
Figure S3. Correlations between the concentrations of **(a)** PAHs and *n*-alkanes **(b)** PAHs and hopanes/steranes **(c)** aromatic acids and phthalates/PAHs **(d)** hopanes and steranes.

61
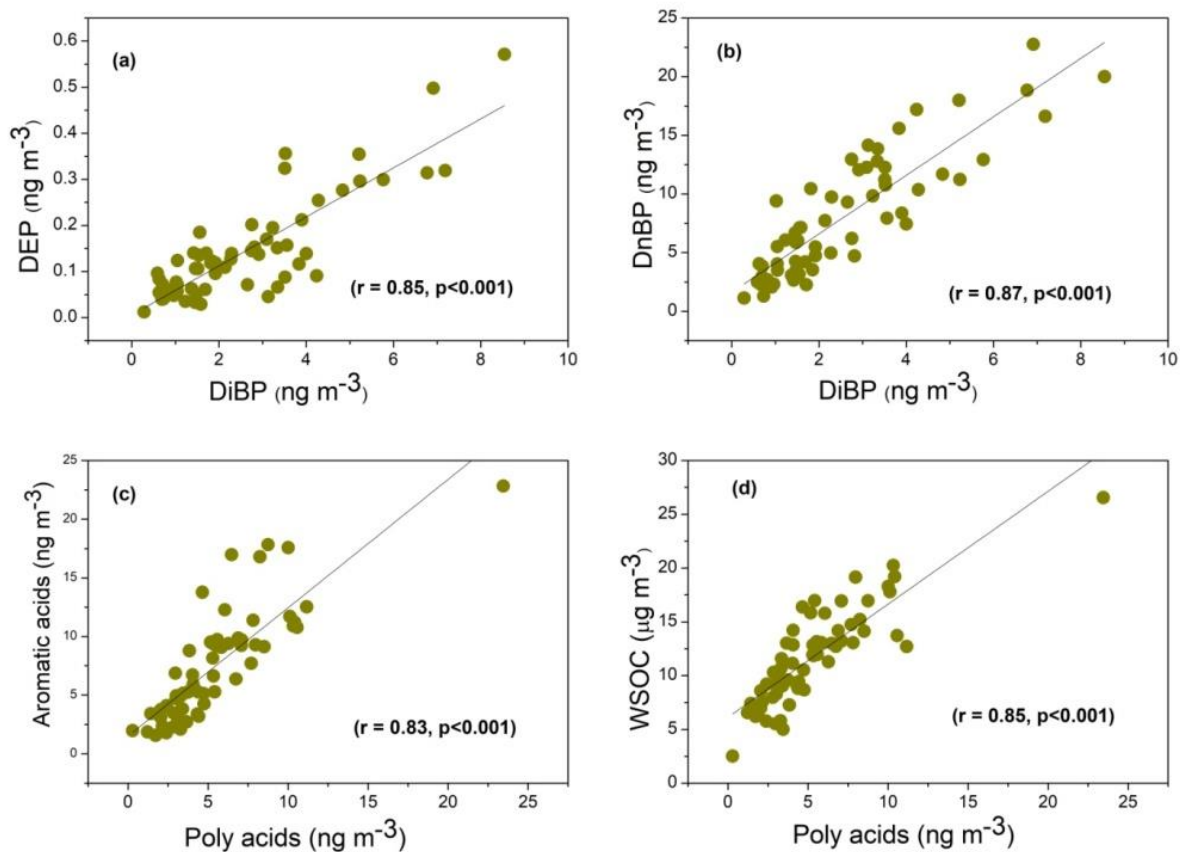
Figure S4. Relationships between the concentrations of **(a)** DiBP (di-iso-butyl phthalate) and DEP (diethyl phthalate) **(b)** DiBP (di-iso-butyl phthalate) and DnBP (di-n-butyl phthalate) **(c)** poly acids and aromatic acids **(d)** poly acids and WSOC.
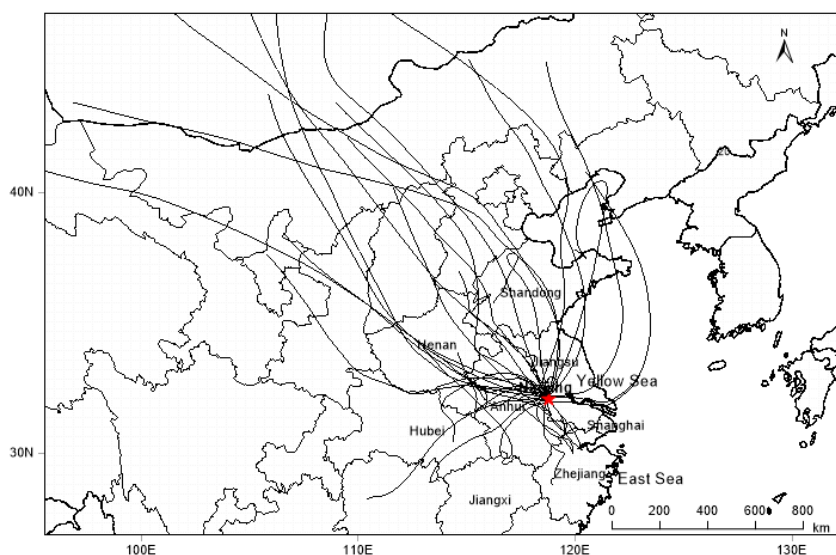
Figure S5. 48 hrs backward air mass trajectories arriving at 500 m above the ground level to Nanjing, China during 11 Dec 2014–11 Jan 2015.